

Joint Sampling and Reconstruction of Time-Varying Signals Over Directed Graphs

Zhenlong Xiao , *Member, IEEE*, He Fang , *Member, IEEE*, Stefano Tomasin , *Senior Member, IEEE*, Gonzalo Mateos , *Senior Member, IEEE*, and Xianbin Wang , *Fellow, IEEE*

I. INTRODUCTION

A. Motivation

Abstract—Vertex-domain and temporal-domain smoothness of time-varying graph signals are cardinal properties that can be exploited for effective graph signal reconstruction from limited samples. However, existing approaches are not directly applicable when the signal's frequency occupancy changes with time. Moreover, while e.g., sensor network applications can benefit from directed graph models, the non-orthogonality of the graph eigenvectors can challenge spectral-based signal reconstruction algorithms. In this context, here we consider K -sparse time-varying signals with unknown frequency supports. By exploiting the smoothness of the varying graph frequency supports and employing shift operations over directed graphs, we study joint sampling of multiple varying signals based on Schur decomposition to reconstruct each signal by orthogonal frequency components. Firstly, joint frequency support of the multiple signals is identified by proposing a two-stage Individual-Joint sampling scheme. Based on the estimated frequency support, the GFT coefficients of each signal can be recovered using data collected in individual sampling stage. Greedy algorithms are proposed for vertex set selection and graph shift order selection, which enable a robust signal reconstruction against additive noise. Considering the signals in applications may be approximately K -sparse, we further exploit the samples in both individual and joint sampling stages and investigate the optimal signal reconstruction as a convex optimization problem with adaptive frequency support selection. The proposed optimal sampling and reconstruction algorithms outperform several existing schemes in random network and sensor network data gathering.

Index Terms—Directed graph, frequency domain, graph signal sampling, signal reconstruction, time-varying signals.

DIFFERENT graph signal processing techniques have been developed in recent years to process data characterized by irregular structures. A wide range of new applications such as sensor networks [1], [2], [3], brain networks [4], [5], social networks [6], [7], [8], and machine learning [9] can benefit from these emerging techniques. Due to the fundamental role of sampling in signal processing, sampling of graph signals has attracted considerable interest and shows its applications in sensor data gathering [10], economic networks [11], point cloud processing [12], and Big Data analytics [13], [14], [15], etc.

In sensor network data gathering, the energy of signals may mainly locate at low-frequency components. However, the middle- and high-frequency components may also provide useful information, and they may not all be ignored in signal reconstruction stage. It would be better to recover signals based on the frequency support that has the largest graph Fourier transform (GFT) coefficient magnitudes so that the reconstructed signals will omit the least information for further processing. If we sample and recover each time-varying signal separately, it would be very difficult to estimate the frequency support having the largest GFT coefficient magnitudes by using only a few samples, which may thus limit the reconstruction performance. Observing from sensor network data that the frequency supports with the largest GFT coefficient magnitudes of adjacent signals would vary smoothly, in this article, a joint sampling method is proposed for multiple time-varying graph signals to identify their joint frequency support, and thereafter, optimal reconstruction is studied to recover each signal. Directed graphs are under the consideration to characterize the data transmission over network.

B. Related Works

Graph Fourier transform provides a powerful tool for sampling and recovery of signals over graphs [16], [17]. A signal that is band-limited or K -sparse in graph spectrum domain can be fully reconstructed from its samples. In [18], an optimal sampling technique was proposed for signals with known frequency support. Connection between the spread of a signal over graphs and the spread of its spectrum was studied in [19], based on which the recovery robust against noise was developed,

Manuscript received 27 October 2022; revised 5 April 2023 and 30 May 2023; accepted 4 June 2023. Date of publication 8 June 2023; date of current version 22 June 2023. The associate editor coordinating the review of this manuscript and approving it for publication was Prof. David I Shuman. This work was supported by the National Natural Science Foundation of China under Grant 62271430. (Corresponding author: He Fang.)

Zhenlong Xiao is with the Department of Information and Communication Engineering, School of Informatics, Xiamen University, Xiamen 361005, China (e-mail: zlxiao@xmu.edu.cn).

He Fang is with the School of Electronic and Information Engineering, Soochow University, Soochow 215006, China (e-mail: fanghe@suda.edu.cn).

Stefano Tomasin is with the Department of Information Engineering, University of Padova, 35122 Padova, Italy (e-mail: tomasin@dei.unipd.it).

Gonzalo Mateos is with the Department of Electrical and Computer Engineering, University of Rochester, Rochester, NY 14627 USA (e-mail: gmateos@ece.rochester.edu).

Xianbin Wang is with the Department of Electrical and Computer Engineering, Western University, London, Ontario N6A 5B9, Canada (e-mail: xianbin.wang@uwo.ca).

Digital Object Identifier 10.1109/TSP.2023.3284364

and the blue-noise sampling method was designed to maximize the distance between sampling nodes [20]. A joint design of sampling and quantization [21] and a non-Bayesian estimator based on Cramer-Rao bound [22] were proposed for signal recovery. An efficient sampling scheme were proposed by dividing the signal space into several one-dimensional subspaces and selecting the effective node in the remaining subspace [23]. In these results, signals can be recovered by the estimated GFT coefficients. To inherit the frequency-domain properties of sampled signals, sampling and recovery were studied in spectral domain [24]. However, these results mainly focus on undirected graphs, where the orthogonality of eigenvectors greatly eases signal reconstruction.

The smoothness of graph signals in vertex domain has been exploited for signal recovery. Local-set-based methods [25] and probabilistic sampling algorithms [26] were developed to recover signals with distributed behaviours. In [27], graph spectral proxies were designed to estimate the bandwidth of signal for reconstruction. Based on Neumann series, a low-complexity recovery algorithm was studied in [28]. Kernel-based operators were designed for efficient sampling [29], and a joint vertex-spectral-domain sampling was proposed in [30]. In these methods, graph filters are employed to recover signals. Hence, most of them focus on band-limited signals such that the smoothness property of the signal can be employed.

Since band-limitedness is restrictive for graph signals in real-world scenarios, many efforts have been devoted to relaxing such requirements. The approximately band-limited signal was studied in [31]. Assuming that the graph is bipartite and signal is identically distributed, sampling via maximum spanning trees was studied in [32]. The estimation of power spectra was developed for second-order stationary signals [33], and sampling of K -sparse signals was studied in [34], where the signals and noise are assumed to be zero-mean circular distributions. A Bayesian estimator was studied to recover signals from nonlinear observations [35], however, the probability density function of graph signal is needed.

To further exploit the properties of graph shift operations on signals, aggregation sampling was studied. For local aggregation in sensor networks, shift operations with an undirected graph may be restricted because the bidirectional transmission on a network may be unnecessary and may not always be available. Shift operations over directed graphs may be more practical in these scenarios. Based on successive local aggregations, signals can be sampled on a single vertex [36], where signal can be K -sparse with unknown frequency support. Orthogonal partition selection was proposed [37] to overcome the ill-condition of the Vandermonde matrix in signal reconstruction [36]. However, its frequency support should be known. A randomized local aggregation sampling was proposed in [38], where the frequency support can be unknown but signals and sampling matrix should satisfy the restricted isometry property.

The aforementioned results mainly focus on sampling and reconstruction of a single graph signal and do not account for its relationship to adjacent signals. In real applications, signals could be time-varying and evolve slowly. The relationships between adjacent graph signals can be studied by

autoregressive models [10], [39], [40], kernel methods [41], time-vertex analysis [42], [43], and product graph framework [44]. Such relationships can contribute to the sampling and reconstruction of varying signals. Local properties of temporal difference were developed for signal reconstruction in [45]. Sampling via a joint optimization of sample selection and a sketch of target linear transform was developed [46] based on the stationary nature of the graph signal sequence. A Tikhonov regularization-based recovery was designed based on the smoothness of graph topology and temporal correlations [47]. In [48], [49], [50], varying signals were characterized by Sobolev smoothness. In these results, signals should be band-limited, approximated band-limited, or the frequency support is known.

C. Contributions:

In this article, we consider joint sampling on multiple time-varying signals based on the observations that the frequency supports of adjacent signals vary smoothly in sensor networks, i.e., the consecutive signals share the most frequency components associated with the largest GFT coefficient magnitudes. By performing shift operations on varying signals, we propose a two-stage Individual-Joint sampling scheme for signal reconstruction. In the individual sampling stage, each signal is sampled separately, and the samples will be applied to estimate their GFT coefficients in next steps. Since only a few samples are collected, they are not sufficient for identifying the joint frequency support. Hence, the multiple signals are combined together, and a joint sampling is further performed on the combined signal. The algorithms are firstly developed based on the assumption that the varying signals are strictly K -sparse with unknown frequency support, which are further extended for full-band signals with Gaussian noise that is approximately K -sparse. The contributions are summarized as:

- 1) A two-stage Individual-Joint sampling scheme is proposed for time-varying graph signals based on shift operations over directed graphs for sensor network data gathering. The joint frequency support of the multiple signals can be identified with the aid of data collected in the joint sampling stage, and each noiseless K -sparse signals can be further recovered using the samples collected in the individual sampling stage.
- 2) Greedy algorithms are proposed for vertex set selection and graph shift order selection, which provide a near-smallest vertex set for the sampling of varying signals. Moreover, for noisy signals, the proposed greedy selection algorithms will guarantee a robust signal reconstruction against additive noise.
- 3) For noisy signals, an unbiased reconstruction algorithm is studied, and an adaptive selection of joint frequency support is proposed since a larger number of frequency components in the joint support will bring more noise in the reconstruction while a smaller size of support will omit more information on the true signal. To further improve the performance, an optimal reconstruction algorithm is proposed by considering the signal reconstruction as a convex

optimization problem, where the data collected in both individual and joint sampling stages are fully exploited and the result of joint frequency support identification is explicitly involved.

The remaining part of this article is organized as follows. Section II presents the problem formulation, and Section III investigates the aggregation sampling of a single signal over directed graph. In Section IV, the two-stage Individual-Joint sampling scheme is studied. Greedy sampling of noiseless signals is shown in Section V, and optimal reconstruction of time-varying noisy signals is studied in Section VI. Numerical studies and discussions are presented in Sections VII and VIII concludes this article.

II. NOTATIONS AND PROBLEM FORMULATION

A. Notations and Preliminaries

Notation: Scalars are denoted using lowercase letters, and vectors are defined using bold lowercase letters. We denote matrices using bold uppercase letters, and $(\cdot)^T$ indicates the transpose of (\cdot) . Sets are represented by calligraphic letters, and $|\cdot|$ stands for the cardinality of set (\cdot) .

Define a directed graph by $G = (\mathcal{V}, \mathbf{A})$, where $\mathcal{V} = \{v_1, v_2, \dots, v_N\}$ is the vertex set, N is the number of vertices, and \mathbf{A} is the weighted adjacency matrix. Denote by

$$\mathbf{U} = [\mathbf{u}_1, \mathbf{u}_2, \dots, \mathbf{u}_M] \quad (1)$$

the M time-varying graph signals, where $\mathbf{u}_m = [u_{1,m}, u_{2,m}, \dots, u_{N,m}]^T \in \mathcal{R}^N$ is the m -th signal, and \mathcal{R} is the set of real numbers. We denote shift operation over graphs by graph shift matrix $\mathbf{S} \in \mathcal{R}^{N \times N}$, which can be defined by weighted adjacency matrix or Laplacian matrix. Graph shift matrix can be considered as an extension of the time shift operator in conventional discrete signal processing to graph signals [10], [51]. Denote by \mathbf{u}_m^ℓ the ℓ -th order shift of \mathbf{u}_m , we have

$$\mathbf{u}_m^\ell = [u_{1,m}^\ell, u_{2,m}^\ell, \dots, u_{N,m}^\ell]^T = \mathbf{S}^\ell \mathbf{u}_m, \quad (2)$$

where $u_{n,m}^\ell$ is the ℓ -th order shifted signal of \mathbf{u}_m on v_n .

We focus on directed graphs, where the graph shift matrix may be asymmetric. Given a graph shift matrix \mathbf{S} , there exists a unitary matrix $\mathbf{Q} = [\mathbf{q}_1, \mathbf{q}_2, \dots, \mathbf{q}_N]$ such that

$$\mathbf{S} = \mathbf{Q}\mathbf{T}\mathbf{Q}^T, \quad (3)$$

where

$$\mathbf{T} = \begin{bmatrix} \mathbf{T}_{1,1} & \mathbf{T}_{1,2} & \cdots & \mathbf{T}_{1,m} \\ 0 & \mathbf{T}_{2,2} & \cdots & \mathbf{T}_{2,m} \\ \cdots & \cdots & \ddots & \cdots \\ 0 & 0 & \cdots & \mathbf{T}_{m,m} \end{bmatrix} \quad (4)$$

is an upper quasi-triangular matrix of size $N \times N$. Eq. (3) is a real Schur decomposition of \mathbf{S} [52]. Each \mathbf{T}_{ii} is either a 1-by-1 scalar with real eigenvalue $\mathbf{T}_{i,i} = \lambda_i$ or a 2-by-2 matrix having complex conjugate eigenvalues, i.e., $\mathbf{T}_{i,i} = \begin{bmatrix} \text{Re}(\lambda_i) & \text{Im}(\lambda_i) \\ -\text{Im}(\lambda_i) & \text{Re}(\lambda_i) \end{bmatrix}$. Schur vectors \mathbf{q}_n are referred to as graph

frequency components [53]. Graph Fourier transform [17] of the m -th signal \mathbf{u}_m is defined by

$$\hat{\mathbf{u}}_m = [\hat{u}_{1,m}, \hat{u}_{2,m}, \dots, \hat{u}_{N,m}]^T = \mathbf{Q}^T \mathbf{u}_m, \quad (5)$$

where $\hat{u}_{n,m}$ are GFT coefficients. Inverse GFT is defined by $\mathbf{u}_m = \mathbf{Q}\hat{\mathbf{u}}_m$ to reconstruct signal \mathbf{u}_m from its GFT coefficients.

Denote by $T_{k,n}$ the (k, n) -th entry of \mathbf{T} and by λ_{\max} the eigenvalue of \mathbf{S} with the largest magnitude. The total variation of Schur vector \mathbf{q}_n can be defined by

$$\begin{aligned} TV(\mathbf{q}_n) &= \left\| \mathbf{q}_n - \frac{1}{\|\lambda_{\max}\|} \mathbf{S} \mathbf{q}_n \right\|_1 \\ &= \left\| \mathbf{q}_n - \frac{T_{n,n}}{\|\lambda_{\max}\|} \mathbf{q}_n - \frac{1}{\|\lambda_{\max}\|} \sum_{\substack{k=1 \\ (k \neq n)}}^{n+1} T_{k,n} \mathbf{q}_k \right\|_1. \end{aligned} \quad (6)$$

In the case that $T_{k,n} = 0$, for $k \neq n$, Schur vector \mathbf{q}_n is an eigenvector corresponding to λ_n , where its total variation is the same as the result in [17]. Otherwise, vectors $\mathbf{q}_1, \mathbf{q}_2, \dots, \mathbf{q}_{n-1}$, and \mathbf{q}_{n+1} may contribute to the total variation of \mathbf{q}_n . If $\|\lambda_{\max}\| \gg T_{k,n}$ holds, the total variation can be approximated by $TV(\mathbf{q}_n) \approx \left\| 1 - \frac{\text{Re}(\lambda_n)}{\|\lambda_{\max}\|} \right\|_1 \|\mathbf{q}_n\|_1$. In such cases, Schur vector \mathbf{q}_n and its corresponding eigenvalue λ_n may also provide an insightful frequency interpretation by the total variation definition. The eigenvalues may appear in any order in the diagonal entries $T_{i,i}$, which will thereby result in different Schur decompositions together with different Schur vectors for a given graph shift matrix \mathbf{S} . In this article, we focus on exploiting the orthogonal basis over directed graphs for signal sampling and reconstruction. An optimal Schur decomposition of a directed graph shift matrix may be developed under different application-oriented criteria, which is beyond the scope of this already fully-packed article and will be discussed in a future study.

B. Problem Formulation

In this article, we assume that the graph is static and directed. The signals given in (1) are time-varying with frequency supports vary smoothly. We will study joint sampling of multiple varying signals and optimal reconstruction of each signal based on a subset of samples.

Suppose that all the signals \mathbf{u}_m are K -sparse, i.e., there are at most K nonzero GFT coefficients in vector $\hat{\mathbf{u}}_m$, where $K \ll N$ holds. Each signal \mathbf{u}_m can be recovered from a subset of its samples, and perfect reconstruction of a K -sparse signal requires at least K samples for reconstruction. Denote by

$$\mathcal{S}_m = \{\mathbf{q}_{k_1}, \mathbf{q}_{k_2}, \dots, \mathbf{q}_{k_{|\mathcal{S}_m|}}\} \quad (7)$$

the frequency support of \mathbf{u}_m , by $|\mathcal{S}_m|$ the number of frequency components in the support, and $|\mathcal{S}_m| \leq K$ holds. \mathcal{S}_m can be any subset of $|\mathcal{S}_m|$ frequency components and these need not be the first $|\mathcal{S}_m|$ components. Assume that the frequency supports of M signals in (1) vary smoothly, i.e., the supports of two adjacent signals (e.g., \mathcal{S}_m and \mathcal{S}_{m+1}) share most frequency components and only very few components are different between them.

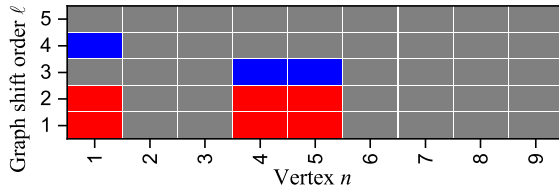


Fig. 1. Sampling in vertex domain and graph shift order domain. Red: the ℓ -th order shifted signal on vertex n will be collected in individual sampling stage, Blue: the ℓ -th order shifted signal on vertex n will be collected in joint sampling stage, Gray: signals will not be selected. The sampling vertex set \mathcal{V}_s and graph shift order set \mathcal{L} are defined in (10) and (11) respectively. There are 9 vertices in the figure, thus we need at least 9 entries (n, ℓ) of signals to estimate the joint frequency support. Each signal is sparse and can thereafter be reconstructed based on much fewer samples collected in individual sampling stage.

Denote the joint frequency support of M signals by \mathcal{S} , i.e.,

$$\mathcal{S} = \mathcal{S}_1 \cup \mathcal{S}_2 \cup \dots \cup \mathcal{S}_M \quad (8)$$

and by $|\mathcal{S}|$ the size of the joint support. We suppose that the combination of multiple signals is also sparse, i.e., $|\mathcal{S}| \ll N$.

From Sections III to V, the time-varying signals are assumed to be strictly K -sparse and noiseless, and in Section VI, noisy signals with additive Gaussian noise are considered, where signals are relaxed to be approximately K -sparse, i.e.,

$$\sum_{k: \mathbf{q}_k \notin \mathcal{S}_m} \|\hat{u}_{k,m}\|^2 \leq \varepsilon \|\hat{\mathbf{u}}_m\|^2 \quad (9)$$

holds with $0 \leq \varepsilon < 1$ a small parameter. That is, the energy associated with the given frequency support \mathcal{S}_m will dominate the energy of signal \mathbf{u}_m . If $\varepsilon = 0$, \mathbf{u}_m is strictly K -sparse.

Denote the sampling vertex set by

$$\mathcal{V}_s = \{v_{n_1}, v_{n_2}, \dots, v_{n_\sigma}\}, \quad (10)$$

where σ is the number of sampling vertices, and by

$$\mathcal{L} = \{\ell_1, \ell_2, \dots, \ell_\tau\} \quad (11)$$

the graph shift order set with $0 \leq \ell_1, \ell_2, \dots, \ell_\tau \leq L$, where L is the given maximum shift order, and τ is the size of \mathcal{L} .

We will study sampling based on local aggregation. As show in Fig. 1, the sampling will be performed in both the vertex domain and the graph shift order domain. If the vertex set \mathcal{V}_s and graph shift order set \mathcal{L} are designed, they will be the same for sampling all the M varying signals. Firstly, each signal will be sampled separately to collect only a few observations, which is referred to as individual sampling stage. Afterward, the M signals are combined and sampling is further performed on the combined signal to help identify the joint frequency support of the multiple signals, which is referred to as the joint sampling stage. Since the joint frequency support that has the largest GFT coefficient magnitudes is identified, the reconstruction of each signal can be conducted based on only a few samples collected during the individual sampling stage. The performance may be better than those existing aggregation based-sampling methods, where the frequency support having the largest GFT coefficient magnitudes is difficult to identify because signals are sampled separately and the joint information of multiple signals is not taken into account for recovering each signal.

Specifically, the problems under consideration will be: 1) How to perform the two-stage Individual-Joint sampling on the M signals? 2) Under what conditions can the multiple signals be perfectly reconstructed? 3) What are the optimal sampling set \mathcal{V}_s and graph shift order set \mathcal{L} for reconstructing each signal? Moreover, 4) how to recover noisy signals in an unbiased fashion and provide optimal reconstruction performance against noise? These problems will be addressed in the following sections.

III. AGGREGATION SAMPLING FOR INDIVIDUAL SIGNAL OVER DIRECTED GRAPHS

In this section, we will focus on sampling and reconstruction of an individual signal \mathbf{u}_m . Since identification of the joint frequency support of multiple signals will be discussed in Section IV-B, we assume that the frequency support \mathcal{S}_m is known for signal \mathbf{u}_m , i.e., the indices k_i of all the non-zero coefficients $\hat{u}_{k_i,m}$ are known for $i = 1, 2, \dots, K$. Frequency support \mathcal{S}_m can be any subset of K frequency components and are unnecessarily to be the first K components.

Aggregation sampling over a single node on directed graphs was discussed in [36], where the graph shift matrix is assumed to be diagonalizable, thus orthogonality of frequency components can not be guaranteed. Orthogonal basis was discussed for signal reconstruction by singular value decomposition of an orthogonal projector [37] or by arbitrarily selecting orthogonal components [38]. For aggregation-based sampling, the samples and reconstruction algorithm would highly associate with the graph shift matrix. Reconstructing signals based on direct orthogonal decomposition of the graph shift matrix would help to characterize the inherent properties of signals associated with the graphs and may thus improve the reconstruction performance. Hence, in the following, we aim to develop sampling algorithms over multiple nodes by employing Schur decomposition, such that the graph frequency components are orthogonal to each other and are directly corresponding to the eigenvalues of the graph shift matrix.

The ℓ -th order shifted signal of \mathbf{u}_m over vertex n is defined in (2), which can be rewritten by

$$\mathbf{u}_{n,m}^\ell = \varphi_n^\ell \hat{\mathbf{u}}_m, \quad (12)$$

where

$$\varphi_n^\ell = \tilde{\mathbf{q}}_n \mathbf{T}^\ell. \quad (13)$$

Vector $\tilde{\mathbf{q}}_n$ is the n -th row of unitary matrix \mathbf{Q} . Perform sampling on the signals shifted up to L -th order (i.e., $\mathbf{u}_m, \mathbf{u}_m^1, \dots, \mathbf{u}_m^L$) over vertex n , and denote by

$$\mathbf{u}_{n,m} = [u_{n,m}, u_{n,m}^1, \dots, u_{n,m}^L]^\top \quad (14)$$

the samples of \mathbf{u}_m over vertex n . The reconstruction matrix for vertex n is defined by

$$\Phi_n = [(\varphi_n^0)^\top, (\varphi_n^1)^\top, \dots, (\varphi_n^L)^\top]^\top \quad (15)$$

of size L -by- N . Samples on vertex n can be formulated by

$$\mathbf{u}_{n,m} = \Phi_n \hat{\mathbf{u}}_m. \quad (16)$$

GFT coefficients $\hat{\mathbf{u}}_m$ can be estimated by samples $\mathbf{u}_{n,m}$.

For signal \mathbf{u}_m , by performing the L -th order shift over graphs and sampling the shifted signals over set \mathcal{V}_s , we can build the reconstruction matrix

$$\Phi = [\Phi_{n_1}^T, \Phi_{n_2}^T, \dots, \Phi_{n_\sigma}^T]^T, \quad (17)$$

which is of size $\sigma L \times N$, and Φ_{n_i} is the reconstruction matrix defined over vertex v_{n_i} for $i = 1, 2, \dots, \sigma$.

Define a frequency selection matrix Ψ of size $K \times N$ to extract all the nonzero GFT coefficients in vector $\hat{\mathbf{u}}_m$, where the (i, k_i) entry $\Psi_{i, k_i} = 1$ holds for $i = 1, 2, \dots, K$, and all the other entries are 0. Hence, we have

$$\hat{\mathbf{u}}_m^K = \Psi \hat{\mathbf{u}}_m, \quad (18)$$

where $\hat{\mathbf{u}}_m^K$ consists of all the nonzero GFT coefficients of $\hat{\mathbf{u}}_m$.

By sampling shifted signals of \mathbf{u}_m on set \mathcal{V}_s , we have

$$\mathbf{u}_m^s = [\mathbf{u}_{n_1, m}^T, \mathbf{u}_{n_2, m}^T, \dots, \mathbf{u}_{n_\sigma, m}^T]^T, \quad (19)$$

which is of size $\sigma L \times 1$. Denote by \mathbf{C} of size $K \times \sigma L$ a joint selection matrix over Φ for selecting vertex and graph shift order, where the entries $\mathbf{C}(i, j) \in 0, 1$, $\sum_{i=1}^K \mathbf{C}(i, j) \leq 1$ hold for all columns, and $\sum_{j=1}^{\sigma L} \mathbf{C}(i, j) = 1$ hold for all rows. \mathbf{u}_m can be reconstructed as follows.

Lemma 1: For aggregation sampling over directed graphs on multiple vertices, we define a square matrix Φ^K of size K -by- K as

$$\Phi^K = \mathbf{C} \Phi \Psi^T. \quad (20)$$

If the number of samples (the row size of Φ) $\sigma L \geq K$ holds, and matrix Φ^K is invertible, the nonzero GFT coefficient vector $\hat{\mathbf{u}}_m^K$ can be estimated by

$$\hat{\mathbf{u}}_m^K = (\Phi^K)^{-1} \mathbf{C} \mathbf{u}_m^s. \quad (21)$$

Signal \mathbf{u}_m can be reconstructed by orthogonal Schur vectors

$$\mathbf{u}_m = \mathbf{Q} \Psi^T \hat{\mathbf{u}}_m^K. \quad (22)$$

Proof: The proof is given in Appendix A. \square

If the support is known for each signal, sampling and reconstruction of multiple signals can be implemented separately for each signal by Lemma 1, where perfect reconstruction of the K -sparse signal uses only a subset of samples. However, frequency support may be varying and be difficult to predict for a new signal in applications. For unknown support problem, to ensure a correct and perfect recovery, we need to estimate all the GFT coefficients, i.e., $\hat{\mathbf{u}}_m^K$ should be replaced by $\hat{\mathbf{u}}_m^N$, and N samples are needed. Hence, Lemma 1 is not applicable for unknown frequency support problems.

Remark 1: We applied Schur decomposition in Lemma 1 for signal sampling and recovery, where frequency components in (3) are orthogonal to each other. To be specific, $(\hat{u}_{k_1, m} \mathbf{q}_{k_1})^T \mathbf{q}_{k_2} = 0$ holds if $k_1 \neq k_2$. However, this identity does not hold for non-orthogonal frequency components based on eigen-decomposition or Jordan decomposition of directed graph shift matrix. For varying frequency supports, the support may not always be correctly identified. If \mathbf{q}_{k_1} is not selected in the support, its signal components will adversely affect the estimation of GFT coefficients of all the other frequency components in the support. For noisy signals, the GFT coefficient estimation

of one frequency component may be perturbed by the noise on all the other frequency components. Hence, orthogonal basis based on Schur vectors may provide better performance in signal recovery, especially when the frequency support is unknown or cannot be perfectly identified.

IV. JOINT SAMPLING OF MULTIPLE SIGNALS AND RECONSTRUCTION WITH UNKNOWN FREQUENCY SUPPORT

In this section, we will study the sampling and reconstruction of multiple time-varying signals with unknown support. The sampling of multiple signals is designed as a two-stage scheme. Firstly, in Section IV-A, an individual sampling stage is presented to collect samples separately for each signal, and in Section IV-B, joint sampling of multiple signals is proposed to collect more samples for identifying the joint frequency support of the multiple signals.

A. Individual Sampling for Graph Signal Reconstruction

Define \mathcal{S}_I to indicate the samples collected in individual sampling stage. If $\mathcal{S}_I(n, \ell) = 1$, the ℓ -th order shifted signal over vertex n , i.e., $u_{n, m}^\ell$, will be collected separately for signal \mathbf{u}_m . \mathcal{L}_I is the graph shift order set for individual sampling. If $\mathcal{S}_I(n, \ell) = 1$, then we define $\ell \in \mathcal{L}_I$. If the joint frequency support \mathcal{S} is identified, we only need $|\mathcal{S}|$ samples to perfectly reconstruct each signal. The sampling set \mathcal{V}_s and graph shift order set \mathcal{L}_I for individual signal should be specifically designed such that $\sigma |\mathcal{L}_I| \geq |\mathcal{S}|$ holds. The minimum size of individual sampling set $|\mathcal{L}_I|$ is given by

$$|\mathcal{L}_I| = \lceil |\mathcal{S}| / \sigma \rceil, \quad (23)$$

where $\lceil \cdot \rceil$ is the ceiling function. The construction of \mathcal{S}_I and estimation of joint frequency support \mathcal{S} will be discussed in Sections V-B and IV-B, respectively.

For individual signal reconstruction, the reconstruction matrix is defined by

$$\Phi^{\mathcal{L}_I} = [(\Phi_{n_1}^{\mathcal{L}_I})^T, (\Phi_{n_2}^{\mathcal{L}_I})^T, \dots, (\Phi_{n_\sigma}^{\mathcal{L}_I})^T]^T, \quad (24)$$

where

$$\Phi_n^{\mathcal{L}_I} = [(\varphi_n^{\ell_1})^T, (\varphi_n^{\ell_2})^T, \dots, (\varphi_n^{\ell_{|\mathcal{L}_I|}})^T]^T, \quad (25)$$

$\ell_i \in \mathcal{L}_I$, and $n = n_1, n_2, \dots, n_\sigma$. The signals over sampling set are collected as

$$\mathbf{u}_m^{s, \mathcal{L}_I} = [(\mathbf{u}_{n_1, m}^{\mathcal{L}_I})^T, (\mathbf{u}_{n_2, m}^{\mathcal{L}_I})^T, \dots, (\mathbf{u}_{n_\sigma, m}^{\mathcal{L}_I})^T]^T \quad (26)$$

with

$$\mathbf{u}_{n, m}^{\mathcal{L}_I} = [u_{n, m}^{\ell_0}, u_{n, m}^{\ell_1}, \dots, u_{n, m}^{\ell_{|\mathcal{L}_I|}}]^T. \quad (27)$$

According to Lemma 1, we have $\mathbf{u}_m^s = \Phi \Psi^T \hat{\mathbf{u}}_m^K$ and

$$\mathbf{u}_m^{s, \mathcal{L}_I} = \Phi^{\mathcal{L}_I} \Psi_{|\mathcal{S}|}^T \hat{\mathbf{u}}_m^{|\mathcal{S}|} \quad (28)$$

for $m = 1, 2, \dots, M$, where $\Psi_{|\mathcal{S}|}$ is a frequency selection matrix of size $|\mathcal{S}| \times N$ to select all the $|\mathcal{S}|$ non-zero coefficients $\hat{\mathbf{u}}_m^{|\mathcal{S}|}$ from $\hat{\mathbf{u}}_m$. Hence, $\hat{\mathbf{u}}_m^{|\mathcal{S}|}$ can be estimated based on the collected samples $\mathbf{u}_m^{s, \mathcal{L}_I}$, and each graph signal \mathbf{u}_m can afterward be

perfectly reconstructed by

$$\mathbf{u}_m = \mathbf{Q}\Psi_{|\mathcal{S}|}^T \hat{\mathbf{u}}_m^{|\mathcal{S}|}. \quad (29)$$

B. Joint Sampling of Multiple Signals for Joint Frequency Support Identification

In this section, we will study support identification by joint sampling on multiple signals to enable perfect reconstruction of K sparse signals using only a few samples.

For each signal \mathbf{u}_m , the samples in individual sampling stage are not sufficient for identifying the joint frequency support since N samples are needed for correctly identifying the joint support \mathcal{S} . We combine the M samples together over vertex v_n for $\mathcal{S}_I(n, \ell) = 1$, i.e.,

$$u_n^\ell = \sum_{m=1}^M u_{n,m}^\ell. \quad (30)$$

Then, the combined signals are defined by

$$\mathbf{u}_n^{\mathcal{L}_I} = [u_n^{\ell_1}, \dots, u_n^{\ell_{|\mathcal{L}_I|}}]^T. \quad (31)$$

Joint sampling is further performed on combined signal u_n^ℓ . Define \mathcal{S}_J to indicate the joint samples, i.e., joint sampling is performed if $\mathcal{S}_J(n, \ell) = 1$, and the corresponding shift order set is denoted by \mathcal{L}_J . The combined samples over v_n are defined by

$$\mathbf{u}_n^{\mathcal{L}_J} = [u_n^{\ell_1}, \dots, u_n^{\ell_{|\mathcal{L}_J|}}]^T, \quad (32)$$

and the reconstruction matrix is given by

$$\Phi_n^{\mathcal{L}_J} = [(\varphi_n^{\ell_1})^T, (\varphi_n^{\ell_2})^T, \dots, (\varphi_n^{\ell_{|\mathcal{L}_J|}})^T]^T \quad (33)$$

for $\mathcal{S}_J(n, \ell_j) = 1$. Samples on v_n are denoted by

$$\mathbf{u}_n^{\mathcal{L}} = [(\mathbf{u}_n^{\mathcal{L}_I})^T, (\mathbf{u}_n^{\mathcal{L}_J})^T]^T, \quad (34)$$

and samples over the whole vertex set \mathcal{V}_s are given by

$$\mathbf{u}^{s, \mathcal{L}} = [(\mathbf{u}_{n_1}^{\mathcal{L}})^T, (\mathbf{u}_{n_2}^{\mathcal{L}})^T, \dots, (\mathbf{u}_{n_\sigma}^{\mathcal{L}})^T]^T, \quad (35)$$

having the reconstruction matrix over vertex n defined by

$$\Phi_n^{\mathcal{L}} = [(\Phi_n^{\mathcal{L}_I})^T, (\Phi_n^{\mathcal{L}_J})^T]^T. \quad (36)$$

Combine the samples \mathbf{u}_m^s given in (19) by

$$\mathbf{u}^s = \sum_{m=1}^M \mathbf{u}_m^s, \quad (37)$$

and define the combined GFT coefficients by

$$\hat{\mathbf{u}} = \sum_{m=1}^M \hat{\mathbf{u}}_m. \quad (38)$$

Denote by \mathbf{C}_N the joint selection matrix of size N -by- σL to select the samples $\mathbf{u}^{s, \mathcal{L}}$ from \mathbf{u}^s , i.e.,

$$\mathbf{u}^{s, \mathcal{L}} = \mathbf{C}_N \mathbf{u}^s, \quad (39)$$

where \mathbf{C}_N has similar definition as \mathbf{C} , and they are only of different sizes. Then, we have

$$\mathbf{u}^{s, \mathcal{L}} = \Phi^N \hat{\mathbf{u}}, \quad (40)$$

where

$$\Phi^N = \mathbf{C}_N \Phi = [(\Phi_{n_1}^{\mathcal{L}})^T, (\Phi_{n_2}^{\mathcal{L}})^T, \dots, (\Phi_{n_\sigma}^{\mathcal{L}})^T]^T. \quad (41)$$

Then, the joint frequency support of the multiple signals can be identified as follows.

Proposition 1: Perform joint sampling on the combined shifted signals over vertex set \mathcal{V}_s , if matrix Φ^N is invertible, the combined GFT coefficients $\hat{\mathbf{u}}$ can be estimated by

$$\hat{\mathbf{u}} = (\Phi^N)^{-1} \mathbf{u}^{s, \mathcal{L}}. \quad (42)$$

Locating all the $|\mathcal{S}|$ non-zero GFT coefficients in $\hat{\mathbf{u}}$ and selecting their corresponding graph frequency components, the joint frequency support can be identified. To uniquely estimate the joint frequency support, the graph shift order satisfies

$$L \geq \lceil N/\sigma \rceil, \quad (43)$$

where $\lceil \cdot \rceil$ is the ceiling function.

Proof: The proof is shown in Appendix B. \square

The two-stage Individual-Joint sampling and reconstruction of M varying signals are summarized in Algorithm 1. If the samples in $\mathbf{u}^{s, \mathcal{L}}$ are obtained, the joint frequency support of the multiple signals can be identified by Proposition 1. The number of frequency components for recovering each signal is reduced to be $|\mathcal{S}|$. Hence, each signal can be perfectly reconstructed by (28)–(29) using only $|\mathcal{S}|$ samples.

Remark 2: In the proposed joint sampling and reconstruction scheme, to ensure that each signal can be perfectly reconstructed, the amount of collected samples is $(M-1)|\mathcal{S}| + N$, where $M|\mathcal{S}|$ is the number of samples in individual sampling stage, and $N - |\mathcal{S}|$ is the number of samples in joint sampling stage over the combined signal. The compression performance of the proposed joint sampling scheme is given as

$$\rho = \frac{MN}{(M-1)|\mathcal{S}| + N}. \quad (44)$$

If N and the size of joint support $|\mathcal{S}|$ are given, the compression performance of the proposed scheme approaches $\frac{N}{|\mathcal{S}|}$ when the number of signals M is big enough.

In this section, we show the joint sampling for frequency support identification and individual sampling to recover each signal. We assume that the reconstruction matrices (Φ^N and $\Phi^{\mathcal{L}_I}$) and selection matrices (\mathbf{C}_N , \mathbf{C} , \mathcal{S}_I , and \mathcal{S}_J) are known, and matrices Φ^N and $\Phi^{\mathcal{L}_I}$ are invertible. In next section, we will focus on the optimal vertex set selection for \mathcal{V}_s and graph shift order selection for \mathcal{L} to build reconstruction matrices (Φ^N and $\Phi^{\mathcal{L}_I}$) and selection matrices (\mathbf{C}_N , \mathbf{C} , \mathcal{S}_I , and \mathcal{S}_J).

V. GREEDY SAMPLING OF NOISELESS SIGNALS OVER DIRECTED GRAPHS

In this section, we will determine the optimal sampling vertex set \mathcal{V}_s and graph shift order set (\mathcal{L}_I and \mathcal{L}_J) for graph signal sampling and reconstruction. Since both the vertex set and graph shift order set are considered, the sampling problem is a two-dimensional combinational problem as shown in Fig. 1. To simplify the optimal sampling, we will cast the problem to be a two-stage one-dimensional selection problem and design

Algorithm 1: Individual-Joint Sampling and Reconstruction for Multiple Time-Varying Graph Signals.

Input: Selection matrices \mathcal{S}_I and \mathcal{S}_J (constructed by (57) and (61)), graph signals \mathbf{u}_m for $m = 1, 2, \dots, M$.

Individual Sampling:

For each graph signal \mathbf{u} , if $\mathcal{S}_I(n, \ell) = 1$, collect samples over vertex n on the shifted signals \mathbf{u}_m^ℓ for $m = 1, 2, \dots, M$.

Collect samples and construct vector \mathbf{u}_m^s defined in (19).

Joint Sampling:

Combine the shifted signals \mathbf{u}_m^ℓ in the *Individual Sampling* stage if $\mathcal{S}_I(n, \ell) = 1$ using (30).

If $\mathcal{S}_J(n, \ell) = 1$, collect samples on the combined signals \mathbf{u}^ℓ , and construct the vector $\mathbf{u}^{s, \mathcal{L}}$ given in (35).

Identification of Joint Frequency Support:

Identify the joint frequency support of the combined signal by Proposition 1.

Reconstruction of Each Graph Signal:

Reconstruct each signal \mathbf{u}_m using the data collected in *Individual Sampling* stage by (28)–(29).

corresponding greedy algorithms. Specifically, we will focus on vertex set selection in Section V-A to build an invertible matrix Φ^N for identifying the joint frequency support, and thereafter, we will study graph shift order set selection in Section V-B to construct matrix $\Phi^{\mathcal{L}_I}$ for perfect recovery of each signal. Big sizes of sampling set \mathcal{V}_s and \mathcal{L} may provide ideal performance for signal reconstruction. However, the corresponding compression performance (44) would deteriorate. Hence, the greedy algorithms will aim at providing approximate smallest sampling sets for \mathcal{V}_s and \mathcal{L}_I .

A. Greedy Vertex Set Selection

In this section, we aim at designing the approximate smallest sampling vertex set \mathcal{V}_s with a given maximum graph shift order L such that reconstruction matrix Φ^N is invertible, i.e.,

$$\min |\mathcal{V}_s| \text{ s.t. } \Phi^N \text{ is invertible.} \quad (45)$$

Assume that a temporary sampling vertex set is given as $\mathcal{V}_{temp} = \{v_{n_1}, v_{n_2}, \dots, v_{n_{temp}}\}$ with the reconstruction matrix defined by

$$\Phi_{temp} = [\Phi_{n_1}^T, \Phi_{n_2}^T, \dots, \Phi_{n_{temp}}^T]^T, \quad (46)$$

which is of size n_t -by- N , and Φ_n is defined in (15). New vertices are to be selected for constructing matrix Φ^N . To reduce the number of sampling vertices, a new vertex v_n to be selected in the sampling set should provide the most independent vectors to the matrix Φ_{temp} . A greedy algorithm is developed for sampling set selection as follows.

Greedy Sampling Vertex Set Selection: For any vertex $v_n \in \mathcal{V} - \mathcal{V}_{temp}$, perform singular value decomposition on

$$\Phi_{temp'} = [\Phi_{temp}^T, \Phi_n^T]^T. \quad (47)$$

Denote by r_{\min} the minimum singular value of $\Phi_{temp'}$, by r_0 a pre-determined threshold, and by $n_{t'}$ the number of singular values of $\Phi_{temp'}$ that are bigger than r_0 .

We choose the vertex v_n if its value $n_{t'}$ is the biggest among the vertex set $\mathcal{V} - \mathcal{V}_{temp}$, and

$$\mathcal{V}_{temp'} = \mathcal{V}_{temp} \cup \{v_n\}. \quad (48)$$

For the new reconstruction matrix, since not all of the singular values are bigger than r_0 , we further define submatrices Φ'_n by selecting $n_{t'} - n_t$ rows from Φ_n , and updating matrix by

$$\Phi_{temp'} = [\Phi_{temp}^T, (\Phi'_n)^T]^T, \quad (49)$$

which is of size $n_{t'}$ -by- N . We choose the submatrix Φ'_n that results in the minimum condition number of $\Phi_{temp'}$ among all the $C_L^{n_{t'} - n_t}$ matrices Φ'_n . The new reconstruction matrix is obtained by (49), and vertex selection matrix is given by

$$C_N(n_t + i, I_n^\ell) = 1 \quad (50)$$

for $i = 1, 2, \dots, n_{t'} - n_t$, where I_n^ℓ is the row index of the selected vector φ_n^ℓ in matrix Φ .

Proposition 2: By selecting a new vertex n according to (47)–(50), the greedy sampling set selection ends when there are N rows in matrix $\Phi_{temp'}$. Hence, we have $\Phi^N = \Phi_{temp'}$ and $\mathcal{V}_s = \mathcal{V}_{temp'}$. If vector φ_n^ℓ is selected in Φ^N , order ℓ will be included in the graph shift order set \mathcal{L} . Since the minimum singular value of Φ^N is bigger than a pre-determined threshold, Φ^N is guaranteed to be invertible after sampling vertex set selection.

Proof: For the selected vertex v_n , there are at least $n_{t'}$ independent components because in (47) we have $n_{t'}$ singular values bigger than the pre-designed threshold r_0 . Hence, there exists at least one submatrix Φ'_n such that the matrix $\Phi_{temp'}$ in (49) is full-rank, and we choose the matrix $\Phi_{temp'}$ that has the minimum condition number. Since new matrix $\Phi_{temp'}$ is full-rank, it is invertible if $\Phi_{temp'}$ is a square matrix. The vertex selection matrix C_N can be built step-by-step after selecting a new vertex. This completes the proof. \square

Remark 3: Since sampling set selection is a combinational problem, it is difficult to guarantee that the size of \mathcal{V}_s is the smallest for matrix Φ^N . For the proposed greedy sampling set selection algorithm, in each step, we select the vertex v_n that can provide the most independent frequency components to the matrix $\Phi_{temp'}$, which can be considered as selecting a new vertex v_n to maximize the rank of new reconstruction matrix $\Phi_{temp'}$ in (49). Note that rank function is a submodular set function. Such a greedy vertex selection algorithm satisfies the submodular property and may make the size of \mathcal{V}_s close to the true minimum value. The second aspect of “greedy” in the proposed algorithm is that we always select the submatrix Φ'_n that makes the temporary reconstruction matrix $\Phi_{temp'}$ having the smallest condition number among all possible matrices.

Once the vertex set for building the reconstruction matrix Φ^N has been selected, the selection matrix C_N can also be obtained. Then, the joint frequency support of the multiple signals can be identified by (42). Since the graph signals are sparse, we can reconstruct each signal using much fewer samples based on $\Phi^{\mathcal{L}_I}$, which will be studied in the following.

B. Graph Shift Order Set Selection

If the joint frequency support has been identified, the frequency selection matrix $\Psi_{|\mathcal{S}|}$ can be designed to extract all the $|\mathcal{S}|$ nonzero GFT coefficients such that we only need $|\mathcal{S}|$ samples to perfectly reconstruct each signal. The matrix $\Phi^{\mathcal{L}_I}$ can be constructed by specifically designing a selection matrix $C_{|\mathcal{S}|}$ to guarantee that matrix $\Phi^{\mathcal{L}_I}$ has full rank. The graph shift order selection problem can be modelled by

$$\min |\mathcal{L}_I| \quad \text{s.t.} \quad \text{rank}(\Phi^{\mathcal{L}_I} \Psi_{|\mathcal{S}|}^T) = |\mathcal{S}|. \quad (51)$$

With the reconstruction vector φ_n^ℓ given in (13), we define the ℓ -th order shift matrix as

$$\Phi^\ell = [(\varphi_{n_1}^\ell)^T, (\varphi_{n_2}^\ell)^T, \dots, (\varphi_{n_\sigma}^\ell)^T]^T \quad (52)$$

to extract all the ℓ -th order shift vectors in Φ^N , which is of size $n_\ell \times N$. Denote by

$$\bar{\Phi}_{temp} = [(\Phi^{\ell_1})^T, (\Phi^{\ell_2})^T, \dots, (\Phi^{\ell_{temp}})^T]^T \quad (53)$$

the temporary reconstruction matrix of size n_ℓ -by- $|\mathcal{S}|$ with

$$\bar{\Phi}^\ell = \Phi^\ell \Psi_{|\mathcal{S}|}^T, \quad (54)$$

and $\mathcal{L}_{I_temp} = \{\ell_1, \ell_2, \dots, \ell_{temp}\}$. To minimize the size of graph shift order set \mathcal{L}_I , we aim at selecting a new matrix $\bar{\Phi}^\ell$ that can provide the most independent rows to matrix $\bar{\Phi}_{temp}$. For $\ell \in \mathcal{L} - \mathcal{L}_{I_temp}$, perform SVD decomposition on matrix

$$\bar{\Phi}_{temp'} = [\bar{\Phi}_{temp}^T, (\bar{\Phi}^\ell)^T]^T. \quad (55)$$

Denote by r_{\min} the minimum singular value of $\bar{\Phi}_{temp'}$, and by $n_{\ell'}$ the number of singular values that are bigger than r_0 , where r_0 is a pre-determined threshold. Then, the matrix $\bar{\Phi}^\ell$ that leads to the maximum $n_{\ell'}$ will be selected.

Define matrix $\bar{\Phi}_{sub}^\ell$ to choose $n_{\ell'} - n_\ell$ rows from $\bar{\Phi}^\ell$, and update the temporary matrix $\bar{\Phi}_{temp'}$ by

$$\bar{\Phi}_{temp'} = [\bar{\Phi}_{temp}^T, (\bar{\Phi}_{sub}^\ell)^T]^T. \quad (56)$$

Select the matrix $\bar{\Phi}_{sub}^\ell$ that results in the minimum condition number among all the $C_{n_{\ell'} - n_\ell}^{n_{\ell'} - n_\ell}$ different matrices $\bar{\Phi}_{temp'}$, where n_ℓ is the row size of $\bar{\Phi}_{sub}^\ell$. Then, for $i = 1, 2, \dots, (n_{\ell'} - n_\ell)$, we update the selection matrix by

$$S_I(n_i, \ell) = 1, \quad (57)$$

$C_{|\mathcal{S}|}(n_\ell + i, \bar{I}_{n_i}^\ell) = 1$ with $\bar{I}_{n_i}^\ell$ is the row index of vector $\varphi_{n_i}^\ell$ in matrix Φ^N , and $\mathcal{L}_{I_temp} = \mathcal{L}_{I_temp} \cup \{\ell\}$.

This process ends when reconstruction matrix $\bar{\Phi}_{temp'}$ is a square matrix of size $|\mathcal{S}| \times |\mathcal{S}|$. We have $\mathcal{L}_I = \mathcal{L}_{I_temp}$, $\bar{\Phi}^{\mathcal{L}_I} = \bar{\Phi}_{temp'}$ and

$$C = C_{|\mathcal{S}|} C_N, \quad (58)$$

where C is the joint selection matrix given in (20). We have

$$\Phi^{\mathcal{L}_I} = C_{|\mathcal{S}|} \Phi^N \quad (59)$$

and

$$\bar{\Phi}^{\mathcal{L}_I} = \Phi^{\mathcal{L}_I} \Psi_{|\mathcal{S}|}^T. \quad (60)$$

In each step, we guarantee that the minimum singular value of matrix $\bar{\Phi}_{temp'}$ is bigger than a predetermined threshold. Hence, $\bar{\Phi}_{temp'}$ is full rank, and matrix $\Phi^{\mathcal{L}_I} \Psi_{|\mathcal{S}|}^T$ is invertible.

After determining reconstruction matrix $\Phi^{\mathcal{L}_I}$, the nonzero GFT coefficients $\hat{u}_m^{|\mathcal{S}|}$ can be estimated by (28), and each graph signal \mathbf{u}_m can be perfectly recovered according to (29). If row vector φ_n^ℓ is included in Φ^N but is not selected in $\Phi^{\mathcal{L}_I}$, it will be involved in $\Phi^{\mathcal{L}_J}$, then,

$$S_J(n, \ell) = 1 \quad (61)$$

holds, and $\mathcal{L}_J = \mathcal{L}_I \cup \{\ell\}$.

Remark 4: In the proposed algorithms, the Schur decomposition of graph shift matrix is needed, and its time complexity is $O(N^3)$. For vertex set selection, to simplify the analysis, we assume that there are k vertices in $\mathcal{V}_{temp'}$ and the size of $\bar{\Phi}_{temp'}$ is kL . The time complexity of SVD decomposition of $\bar{\Phi}_{temp'}$ is $O((kL)^2 N)$. By selecting σ vertices, the total computation is $\sum_{k=1}^{\sigma} (N - k)(kL)^2 N$ resulting in the time complexity of $O(N^2 L^2 \sigma^3)$. The complexity of graph shift order set selection is $O(|\mathcal{S}|^3 L^2)$. The vertex set and graph shift order set can also be designed by random selection, and the complexity would be $O(N^3)$ since only Schur decomposition is needed. If the graph shift matrix S is given and fixed over time, the sampling vertex set and graph shift order set can be determined only once and then be applied to the sampling and reconstruction of different time-varying signals over the time-invariant graph.

VI. OPTIMAL RECONSTRUCTION OF NOISY SIGNALS OVER DIRECTED GRAPH

In this section, an approximately K -sparse signal is considered since a noisy signal may not be strictly K -sparse. Firstly, an unbiased reconstruction algorithm is studied to eliminate the bias caused by noise in graph shift operations. Then, we will show that the proposed greedy sampling in Section V can provide a robust estimation of GFT coefficients against noise. An adaptive frequency support selection method is proposed to provide an appropriate joint frequency support for signal recovery. Finally, signal reconstruction is considered as a convex optimization problem to fully exploit the data collected in both individual sampling and joint sampling stages as well as the result of joint frequency support identification.

A. Unbiased Reconstruction of Noisy Signals

Assume that signal \mathbf{u}_m is corrupted by additive noise, i.e.,

$$\tilde{\mathbf{u}}_m = \mathbf{u}_m + \mathbf{n}_m, \quad (62)$$

where $\mathbf{n}_m \sim \mathcal{N}(\mathbf{0}, \tilde{\sigma}^2 \mathbf{I})$ is the zero-mean additive noise with a covariance matrix $\mathbf{R} = \tilde{\sigma}^2 \mathbf{I}$. Denote $\mathbf{n} = \sum_{m=1}^M \mathbf{n}_m$, which follows $\mathbf{n} \sim \mathcal{N}(\mathbf{0}, M\tilde{\sigma}^2 \mathbf{I})$.

Performing greedy sampling on noisy signals, we have samples $\tilde{\mathbf{u}}^{s, \mathcal{L}}$ for identifying the joint frequency support with

$$\tilde{\mathbf{u}}^{s, \mathcal{L}} = \Phi^N \tilde{\mathbf{u}}, \quad (63)$$

where the noisy GFT coefficients are given by $\tilde{\mathbf{u}} = \hat{\mathbf{u}} + \mathbf{Q}^* \mathbf{n}$. The frequency support can be estimated by selecting the $|\mathcal{S}|$ frequency components that correspond to the largest magnitudes

in $\tilde{\mathbf{u}}$. Noisy samples $\tilde{\mathbf{u}}_m^{s,\mathcal{L}_I}$ can be used to reconstruct each graph signal by

$$\tilde{\mathbf{u}}_m^{s,\mathcal{L}_I} = \Phi^{\mathcal{L}_I} \Psi_{|\mathcal{S}|}^T \tilde{\mathbf{u}}_m^{|\mathcal{S}|}, \quad (64)$$

where the noisy GFT coefficients are given as

$$\tilde{\mathbf{u}}_m^{|\mathcal{S}|} = \hat{\mathbf{u}}_m^{|\mathcal{S}|} + \Psi_{|\mathcal{S}|} \mathbf{Q}^T \mathbf{n}_m. \quad (65)$$

Although the noise \mathbf{n} is assumed to be white noise, the noise observed in collecting samples $\tilde{\mathbf{u}}^{s,\mathcal{L}}$ is colored due to the graph shift operations. The observed noise is given by $\tilde{\mathbf{n}} = \Phi^N \mathbf{Q}^T \mathbf{n}$ with the covariance matrix

$$\mathbf{R}_{\tilde{\mathbf{n}}} = M \tilde{\sigma}^2 \Phi^N (\Phi^N)^T. \quad (66)$$

The unbiased estimation [54] of $\hat{\mathbf{u}}$ is given by

$$\hat{\mathbf{u}}^e = ((\Phi^N)^T \mathbf{R}_{\tilde{\mathbf{n}}}^{-1} \Phi^N)^{-1} (\Phi^N)^T \mathbf{R}_{\tilde{\mathbf{n}}}^{-1} \tilde{\mathbf{u}}^{s,\mathcal{L}}. \quad (67)$$

The joint frequency support can be identified by selecting $|\mathcal{S}|$ frequency components corresponding to the largest magnitudes in $\hat{\mathbf{u}}^e$. Denote by $\tilde{\mathbf{n}}_m$ the noise in the samples for reconstructing each graph signal, i.e.,

$$\tilde{\mathbf{n}}_m = \Phi^{\mathcal{L}_I} \Psi_{|\mathcal{S}|}^T \Psi_{|\mathcal{S}|} \mathbf{Q}^T \mathbf{n}_m, \quad (68)$$

and by $\mathbf{R}_{\tilde{\mathbf{n}}_m}$ the covariance matrix as

$$\mathbf{R}_{\tilde{\mathbf{n}}_m} = \tilde{\sigma}^2 \Phi^{\mathcal{L}_I} \Psi_{|\mathcal{S}|}^T \Psi_{|\mathcal{S}|} (\Phi^{\mathcal{L}_I})^T. \quad (69)$$

The unbiased estimation [54] of $\hat{\mathbf{u}}_{|\mathcal{S}|,m}$ is given by

$$\begin{aligned} \hat{\mathbf{u}}_m^{|\mathcal{S}|,e} &= \left((\Phi^{\mathcal{L}_I} \Psi_{|\mathcal{S}|}^T)^T \mathbf{R}_{\tilde{\mathbf{n}}_m}^{-1} \Phi^{\mathcal{L}_I} \Psi_{|\mathcal{S}|}^T \right)^{-1} \\ &\quad \times (\Phi^{\mathcal{L}_I} \Psi_{|\mathcal{S}|}^T)^T \mathbf{R}_{\tilde{\mathbf{n}}_m}^{-1} \tilde{\mathbf{u}}_m^{s,\mathcal{L}_I}. \end{aligned} \quad (70)$$

Hence, each noisy signal $\tilde{\mathbf{u}}_m$ can be reconstructed unbiasedly.

B. Robust Estimation of Noisy Signals by Greedy Sampling

In constructing matrices Φ^N and $\bar{\Phi}^{\mathcal{L}_I}$, we guarantee that the matrices have minimum condition numbers in each step. For noisy signals, we will show that such a greedy sampling will ensure robust frequency support identification and signal reconstruction against noise. We define relative errors by

$$e_u = \|\hat{\mathbf{u}}^e - \hat{\mathbf{u}}\| / \|\hat{\mathbf{u}}\| \quad (71)$$

and

$$e_{u,m} = \|\hat{\mathbf{u}}_m^{|\mathcal{S}|,e} - \hat{\mathbf{u}}_m^{|\mathcal{S}|}\| / \|\hat{\mathbf{u}}_m^{|\mathcal{S}|}\|, \quad (72)$$

and denote by $\kappa(\cdot)$ the condition number of matrix (\cdot) .

Proposition 3: The greedy sampling of noisy signals will result in robust signal reconstruction against additive noise by providing small error bounds for e_u and $e_{u,m}$ in estimating the GFT coefficients of $\hat{\mathbf{u}}$ and $\hat{\mathbf{u}}_{|\mathcal{S}|,m}$.

Proof: For identifying the joint frequency support via (63), the following inequalities hold [52],

$$e_u = \|\hat{\mathbf{u}}^e - \hat{\mathbf{u}}\| / \|\hat{\mathbf{u}}\| \leq \kappa(\Phi^N) \|\tilde{\mathbf{u}}^{s,\mathcal{L}} - \Phi^N \hat{\mathbf{u}}^e\| / \|\tilde{\mathbf{u}}^{s,\mathcal{L}}\|. \quad (73)$$

For estimating GFT coefficients of signal \mathbf{u}_m , we have

$$e_{u,m} = \frac{\|\hat{\mathbf{u}}_m^{|\mathcal{S}|,e} - \hat{\mathbf{u}}_m^{|\mathcal{S}|}\|}{\|\hat{\mathbf{u}}_m^{|\mathcal{S}|}\|} \leq \kappa(\bar{\Phi}^{\mathcal{L}_I}) \frac{\|\tilde{\mathbf{u}}_m^{s,\mathcal{L}_I} - \bar{\Phi}^{\mathcal{L}_I} \hat{\mathbf{u}}_m^{|\mathcal{S}|,e}\|}{\|\tilde{\mathbf{u}}_m^{s,\mathcal{L}_I}\|}. \quad (74)$$

Smaller condition numbers $\kappa(\Phi^N)$ and $\kappa(\bar{\Phi}^{\mathcal{L}_I})$ will result in smaller relative error bounds for estimating the GFT coefficients in identifying the joint frequency support as well as in reconstructing each signal. Hence, robust signal reconstruction can be obtained against noise. This completes the proof. \square

C. Adaptive Graph Frequency Support Selection

Although we have already selected $|\mathcal{S}|$ frequency components corresponding to the largest magnitudes in $\hat{\mathbf{u}}^e$ as joint frequency support. For noisy signals, due to the existence of noise \mathbf{n} in the collected samples, the estimated frequency support may not always include all of the true frequency components, which will deteriorate the performance in reconstructing each signal. In the following, optimal signal recovery will be studied by adaptively selecting joint frequency support.

Denote by e_{nrmsc} the normalized root mean square error

$$e_{nrmsc} = 20 \log_{10} \frac{\|\mathbf{u}_m(\mathcal{V}_s) - \mathbf{C}_s \mathbf{Q} \Psi_{|\mathcal{S}|}^T \hat{\mathbf{u}}_m^{|\mathcal{S}|,e}\|}{\|\mathbf{u}_m(\mathcal{V}_s)\|} \quad (75)$$

to evaluate signal reconstruction performance over sampling vertex set \mathcal{V}_s , where $\mathbf{u}_m(\mathcal{V}_s)$ is the signal \mathbf{u}_m over \mathcal{V}_s , and \mathbf{C}_s is the vertex selection matrix to select the reconstructed signals over set \mathcal{V}_s . Define the frequency selection matrix by

$$\bar{\Psi} = \mathbf{I} - \Psi_{|\mathcal{S}|}^T \Psi_{|\mathcal{S}|} \quad (76)$$

to extract all the frequency components that are not selected in the joint frequency support, and the corresponding GFT coefficients $\hat{\mathbf{u}}_r^e$ can be calculated by

$$\hat{\mathbf{u}}_r^e = \bar{\Psi} \hat{\mathbf{u}}^e. \quad (77)$$

After reconstructing each signal, we will evaluate the performance over sampling vertex set \mathcal{V}_s by (75). If the performance is worse than a desired value, the targeted true frequency components may not be involved in the joint frequency support, and the new frequency component corresponding to the largest magnitude in $\hat{\mathbf{u}}_r^e$ will be selected. Once the true components are correctly included in the joint frequency support, the reconstruction performance over sampling vertices will be improved, indicating the optimal reconstruction of signal in terms of small normalized mean square error. Algorithm 2 is summarized to adaptively select joint frequency support.

For noisy signals that may be approximately K -sparse, optimal signal reconstruction will be discussed in next section.

D. Optimal Reconstruction of Each Graph Signal

In this section, we aim at improving the signal reconstruction performance assisted by the frequency components that are not involved in the joint frequency support. The data collected in joint sampling stage as well as the results of joint frequency support estimation can provide additional information to estimate GFT coefficients $\hat{\mathbf{u}}_m$, which may thus contribute to improve the recovery performance.

Using the samples in individual sampling stage, we can estimate the GFT coefficients $\hat{\mathbf{u}}_m$ by dropping the frequency

Algorithm 2: Optimal Reconstruction via Adaptive Frequency Support Selection.

Input: Noisy samples $\tilde{\mathbf{u}}^{s,\mathcal{L}}$ and $\tilde{\mathbf{u}}_m^{s,\mathcal{L}_I}$, desired performance e_d , maximum loop number N_{\max} , and $n = 0$.

Perform unbiased estimation for joint frequency support identification by (67);

Reconstruct each signal unbiasedly by (70), and evaluate its reconstruction performance e_{nrmsc} by (75);

while ($e_{nrmsc} > e_d$) & (& ($n < N_{\max}$))

Select the frequency component corresponding to the largest magnitude in vector \mathbf{u}_r^e defined in (77) to join in the frequency support, and update the frequency selection matrices $\Psi_{|\mathcal{S}|}$ and $\bar{\Psi}$ correspondingly;

Update the reconstruction matrix $\Phi^{\mathcal{L}_I}$ by (60) and noise covariance matrix $\mathbf{R}_{\tilde{n}_m}$ by (69);

Estimate the unbiased GFT coefficients by (70) and evaluate the reconstruction performance e_{nrmsc} by (75);
 $n = n + 1$;

end while

selection matrix $\Psi_{|\mathcal{S}|}$ in (70) as

$$(\Phi^{\mathcal{L}_I})^T \mathbf{R}_{\tilde{n}_m}^{-1} \tilde{\mathbf{u}}_m^{s,\mathcal{L}_I} = (\Phi^{\mathcal{L}_I})^T \mathbf{R}_{\tilde{n}_m}^{-1} \Phi^{\mathcal{L}_I} \tilde{\mathbf{u}}_m, \quad (78)$$

where

$$\mathbf{R}_{\tilde{n}_m} = \tilde{\sigma}^2 \Phi^{\mathcal{L}_I} (\Phi^{\mathcal{L}_I})^T. \quad (79)$$

Rewrite reconstruction matrix on shift order set \mathcal{L}_J by

$$\Phi^{\mathcal{L}_J} = [(\Phi_{n_1}^{\mathcal{L}_J})^T, (\Phi_{n_2}^{\mathcal{L}_J})^T, \dots, (\Phi_{n_\sigma}^{\mathcal{L}_J})^T]^T, \quad (80)$$

and collect the noisy samples in joint sampling stage as

$$\tilde{\mathbf{u}}^{s,\mathcal{L}_J} = [(\tilde{\mathbf{u}}_{n_1}^{\mathcal{L}_J})^T, (\tilde{\mathbf{u}}_{n_2}^{\mathcal{L}_J})^T, \dots, (\tilde{\mathbf{u}}_{n_\sigma}^{\mathcal{L}_J})^T]^T. \quad (81)$$

The noisy GFT coefficients satisfy the following equation,

$$\tilde{\mathbf{u}}^{s,\mathcal{L}_J} = \Phi^{\mathcal{L}_J} \tilde{\mathbf{u}} = \Phi^{\mathcal{L}_J} \hat{\mathbf{u}} + \tilde{\mathbf{n}}^J, \quad (82)$$

where $\tilde{\mathbf{n}}^J = \Phi^{\mathcal{L}_J} \mathbf{Q}^T \mathbf{n}$ with $\mathbf{R}_{\tilde{n}_m}$ the corresponding covariance matrix as

$$\mathbf{R}_{\tilde{n}_m} = M \tilde{\sigma}^2 \Phi^{\mathcal{L}_J} (\Phi^{\mathcal{L}_J})^T. \quad (83)$$

The GFT coefficients can be unbiasedly estimated by

$$(\Phi^{\mathcal{L}_J})^T \mathbf{R}_{\tilde{n}_m}^{-1} \tilde{\mathbf{u}}^{s,\mathcal{L}_J} = (\Phi^{\mathcal{L}_J})^T \mathbf{R}_{\tilde{n}_m}^{-1} \Phi^{\mathcal{L}_J} \tilde{\mathbf{u}}. \quad (84)$$

The unbiased signal reconstruction can afterward be modeled as a convex optimization problem by estimating the GFT coefficients $\hat{\mathbf{u}}_1, \hat{\mathbf{u}}_2, \dots, \hat{\mathbf{u}}_M$ as

$$\min_{\hat{\mathbf{u}}_1, \hat{\mathbf{u}}_2, \dots, \hat{\mathbf{u}}_M} \lambda_1 f_1 + \lambda_2 f_2 + \lambda_3 f_3 + \lambda_4 f_4, \quad (85)$$

where

$$f_1 = \sum_{m=1}^M \|(\Phi^{\mathcal{L}_I})^T \mathbf{R}_{\tilde{n}_m}^{-1} \tilde{\mathbf{u}}_m^{s,\mathcal{L}_I} - (\Phi^{\mathcal{L}_I})^T \mathbf{R}_{\tilde{n}_m}^{-1} \Phi^{\mathcal{L}_I} \hat{\mathbf{u}}_m\|, \quad (86)$$

$$f_2 = \|(\Phi^{\mathcal{L}_J})^T \mathbf{R}_{\tilde{n}_m}^{-1} \tilde{\mathbf{u}}^{s,\mathcal{L}_J} - (\Phi^{\mathcal{L}_J})^T \mathbf{R}_{\tilde{n}_m}^{-1} \Phi^{\mathcal{L}_J} \sum_{m=1}^M \hat{\mathbf{u}}_m\|, \quad (87)$$

$$f_3 = \|\hat{\mathbf{u}}^e - \sum_{m=1}^M \hat{\mathbf{u}}_m\|, \quad (88)$$

$$f_4 = \sum_{m=1}^M \|\bar{\Psi} \hat{\mathbf{u}}_m\|, \quad (89)$$

and $\lambda_i > 0$ for $i = 1, 2, 3, 4$, are the weights of the objectives f_i . In this convex estimation problem, the samples of individual sampling stage contribute to objective f_1 , the data of joint sampling stage is considered in f_2 , the result of joint frequency support identification is included in f_3 , and objective f_4 aims at minimizing GFT coefficients of the components that are not included in the joint frequency support. The weights should be specifically designed for applications. λ_i can be designed according to the error f_i feedback from the collected samples. For example, if error f_i is much greater than the other errors, we may increase the corresponding weight λ_i to increase the proportion of $\lambda_i f_i$ in the weighted total error of (85), which may help to reduce the error f_i .

Remark 5: We assume that the distributions of noise \mathbf{n}_m on each vertex are the same. Since the focus of our algorithms is on sensor data gathering, we can independently measure the data multiple times on very few vertices and estimate the noise variance via sample averaging. If we have certain assumptions on the sensor data, the noise variance can be adaptively estimated in an online fashion using a Kalman filter [55] over each sampled vertex.

Remark 6: For noiseless signals that are approximately K -sparse, model (85)–(89) can also be applied to the joint sampling and reconstruction of varying signals, by denoting $\mathbf{R}_{\tilde{n}_m}^{-1} = \mathbf{I}$ and $\mathbf{R}_{\tilde{n}_m}^{-1} = \mathbf{I}$.

Remark 7: The model (85)–(89) can be considered as an unconstrained linear optimization problem. Hence, the solution with the smallest norm can be solved by weighted least squares [56]. The problem may also be solved by optimization solvers such as CVX [57], [58], where the norm of the GFT coefficients may be considered in (85) by adding $\lambda_5 f_5 = \lambda_5 \sum_{m=1}^M \|\hat{\mathbf{u}}_m\|$ to the objective function.

VII. NUMERICAL STUDIES AND DISCUSSIONS

In this section, two examples (directed random graph and sensor network data gathering) are presented to illustrate the proposed optimal algorithms for joint sampling and recovery of multiple varying signals. In all examples, we assume that the frequency supports of the signals are varying and unknown. The signal reconstruction performance is evaluated by normalized root mean square error defined by

$$P_{\text{NRMSE}} = 20 \log_{10} \frac{\|\mathbf{u}_m - \mathbf{u}_m^{\text{recon}}\|_2}{\|\mathbf{u}_m\|_2}. \quad (90)$$

When signals are reconstructed from noisy samples, we use P_{NRMSE} to measure the closeness between the recovered signal and the true noiseless signal, hence, \mathbf{u}_m therein should be the ground truth noiseless signal.

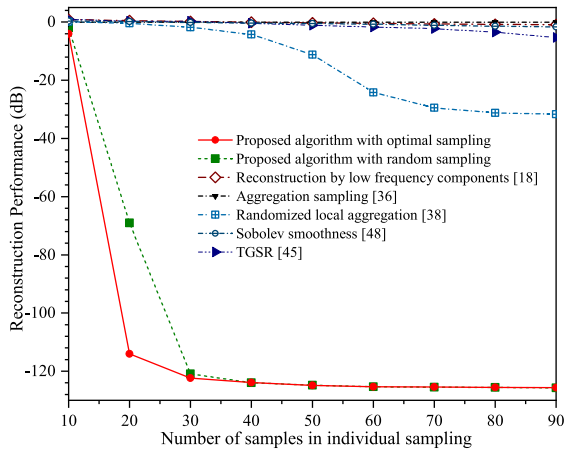


Fig. 2. Noiseless signal reconstruction over random graph with unknown frequency support.

A. Joint Sampling on Directed Random Graph

In this example, directed random graphs with $N = 100$ nodes are studied by including each edge in the graph with probability $p = 0.1$, where the probability of both directions for a given pair of nodes are the same. We perform joint sampling on 3 graph signals, where the joint frequency support of the 3 graph signals is designed by randomly selecting 20 frequency components. The frequency supports of every 3 signals are varying slowly, and each support is a subset of the joint support having 19 frequency components. The GFT coefficients of the signals are randomly generated and from a Gaussian distribution $\mathcal{N}(0, 50)$. The experiments are repeated 100 times with 300 varying signals. The weights are given as $(\lambda_1, \lambda_2, \lambda_3, \lambda_4) = (1, 1, 0.1, 0.1)$.

The average performances for noiseless signals are shown in Fig. 2.¹ We can observe that the proposed algorithm with optimal sampling perfectly recovers the signals if the number of samples in the individual sampling stage is more than 20. If the samples are randomly collected, the performance would be worse when the number of individual samples is not big enough, e.g., less than 30 samples. The aggregation sampling [36] is performed on only one vertex, where the shift matrix is considered by $S_{sym} = 0.5(S + S^T)$ to guarantee that the matrix is diagonalizable. The aggregation sampling only recovers the coefficient of the first frequency component because the ratio of the first two eigenvalues is big in this example, resulting in the case that all the other GFT coefficients are close to 0. The performance can be improved by randomized local aggregation sampling [38] as the ill-conditioned property of the Vandermonde matrix in signal recovery is overcome. The sampling method in [18] is performed based on the low-frequency components since it is unavailable for frequency support unknown problems. It is difficult to provide a good performance because of the incorrect frequency support considered in the reconstruction. The reconstruction based on Sobolev smoothness [48] and temporal

¹The codes are available at <https://github.com/zlxiao-github/JointSamplingOverDirectedGraphs>.

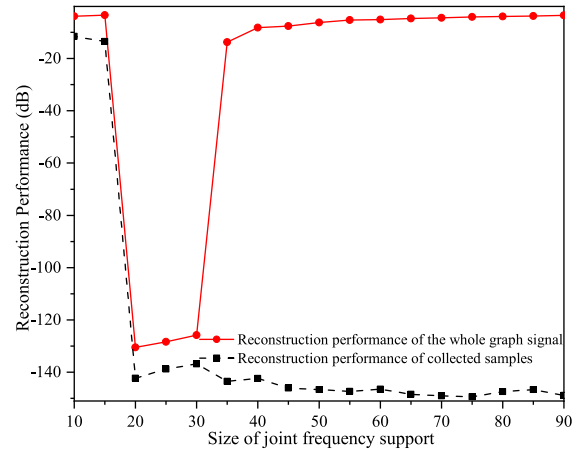


Fig. 3. Optimal reconstruction via adaptive graph frequency support selection.

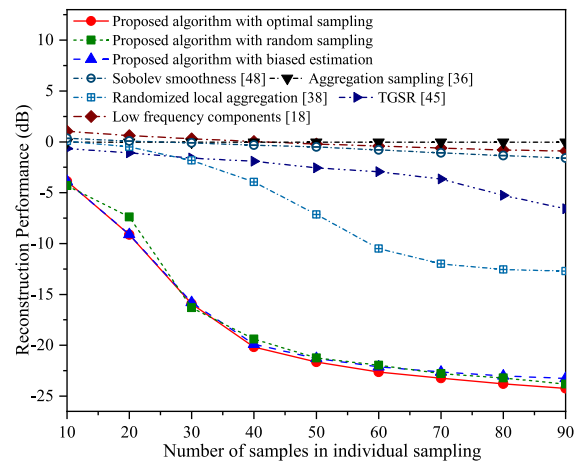


Fig. 4. Noisy signal reconstruction over random graph with unknown frequency support.

difference smoothness [45] do not provide good performances because the varying signals may not be smooth enough.

In Fig. 3, we show the adaptive frequency support selection in the optimal signal reconstruction using 40 individual samples. As the size of joint frequency support increases, the number of GFT coefficients constrained by (89) decreases, and more GFT coefficients can be freely designed in (86)–(88). That is, the complexity of the reconstruction model is higher, and there may exist the so-called over-fitting phenomenon. Firstly, the reconstruction errors of collected samples and the whole signal both decrease. As the size of frequency support increases, we may have too many GFT coefficients to be determined, which could be even bigger than the number of samples. The performance of recovering collected samples improves but that of the whole signal deteriorates. Hence, the size of joint frequency support should be specifically designed using the proposed adaptive selection algorithm.

Additive noise is considered in Fig. 4, where the average signal-to-noise ratio (SNR) is 26 dB. We can observe that as the number of samples increases, the reconstruction performance of

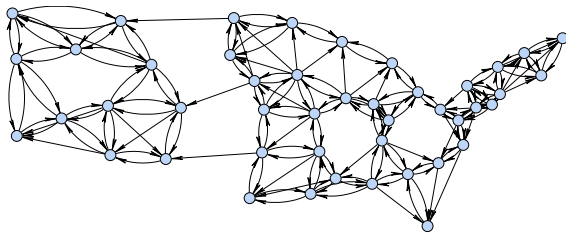


Fig. 5. Directed graph of the US sensor network, where each sensor receives data from 4 nearest neighbour sensors.

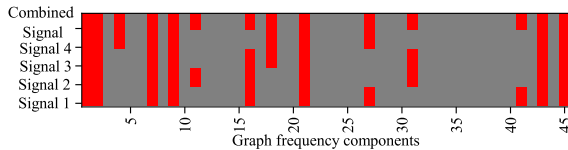


Fig. 6. Graph frequency supports of 4 adjacent signals associated with the 10 largest GFT coefficient magnitudes and the corresponding joint frequency support of the combined signals associated with the 14 largest GFT coefficient magnitudes. Red: frequency components involved in the support. Gray: frequency components that are not selected in the support.

the proposed optimal algorithm improves and would approach to the signal-to-noise ratio of the original signal. When the number of samples is not big enough, e.g., smaller than 40 samples in individual sampling, the proposed greedy vertex set selection together with graph shift order set selection result in smaller errors than randomly sampling. When the number of samples is big, the proposed unbiased reconstruction outperforms the corresponding biased estimation. Similar to the noiseless case, the performances of algorithms in [18], [36], [38], [45], [48] for noisy signals still can be improved.

B. Joint Sampling for Data Gathering in Sensor Networks: Directed Graph With $N = 45$

In this example, the dataset consisting of temperature measurements is borrowed from [59], where the average daily temperatures are collected from $N = 45$ cities in US. We consider the data over 360 days in this example and perform joint sampling on every 4 graph signals. The graph shift matrix is defined based on the locations of sensors by

$$\mathcal{S}(n, m) = e^{-\tilde{d}_{n,m}^2} / \sqrt{\sum_{k \in \mathcal{N}_n} e^{-\tilde{d}_{n,k}^2} \sum_{l \in \mathcal{N}_m} e^{-\tilde{d}_{m,l}^2}}, \quad (91)$$

where $\tilde{d}_{n,m} = d_{n,m}/\eta$, $d_{n,m}$ is the distance between the n -th and m -th sensors, and $\eta = 200$. The neighbor set \mathcal{N}_n will only include 4 nearest neighbour cities of city n , and the other cities will not be involved. The directed graph is shown in Fig. 5, and the weights are given as $(\lambda_1, \lambda_2, \lambda_3, \lambda_4) = (100, 100, 20, 0.1)$.

In Fig. 6, we highlight the frequency components corresponding to the 10 largest GFT coefficient magnitudes of each signal by red, which are selected as the corresponding frequency support of each signal. We can see that the adjacent signals share many components in their frequency supports. The variation of frequency supports of adjacent signals can be considered

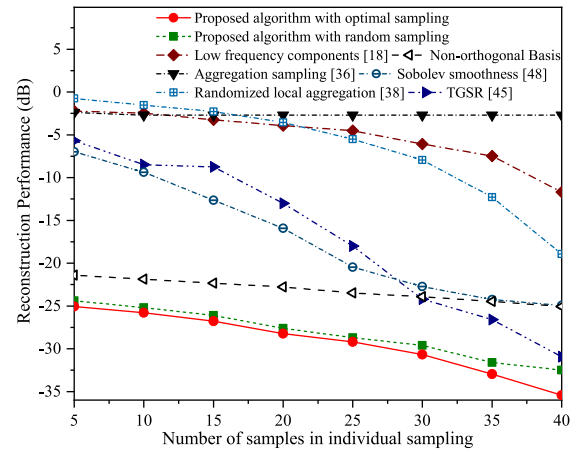


Fig. 7. Noiseless signal reconstruction over US sensor network with unknown frequency support.

as smooth. Since the first 10 frequency components do not always have the largest GFT coefficient magnitudes, signal recovery based on the estimated joint frequency support is able to provide better performance than that based on low frequency components [18].

In Fig. 7, to provide a fair comparison, the number of samples in [18] is the same as that of the proposed joint sampling, i.e., the number of individual samples plus the average number of joint samples for each signal. As the number of samples increases, the reconstruction performance of the proposed optimal algorithm improves. The proposed joint sampling with random selection method is repeated 20 times. Each time selection matrices \mathcal{S}_I and \mathcal{S}_J are randomly generated, and we should guarantee that Φ^N is invertible in random sampling. Based on aggregation sampling method [36], only very few GFT coefficients can be estimated. The performance of Sobolev smoothness-based method [48] is close to the temporal difference smoothness-based method [45]. Eigenvectors of the directed graph shift matrix are applied to the proposed optimal sampling method. The eigen-basis is non-orthogonal, and its performance is worse than that by orthogonal basis when the same weights λ_i are considered.

To demonstrate the performance of unbiased signal reconstruction, Gaussian white noise is added to the temperature measurements in vertex domain with an average SNR of 30 dB. We can observe from Fig. 8 that the more samples collected, the better performance of the proposed unbiased reconstruction can be obtained, which will be close to the SNR of the noisy signal. The optimal reconstruction performance is also better than the biased recovery. The experiments of aggregation sampling, randomized local aggregation, temporal difference smoothness-based method, and Sobolev smoothness-based algorithms are repeated 20 times. Their performances are not better than the proposed optimal reconstruction method. The reason may be that only 4 graph signals are considered in each group and the smoothness property of time-varying signals cannot be well guaranteed for these methods. More signals can be considered to improve the smoothness, however, it may also increase the

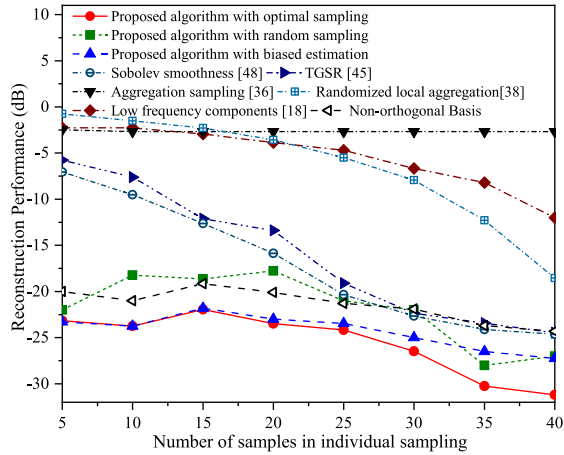


Fig. 8. Noisy signal reconstruction over US sensor network with unknown frequency support.

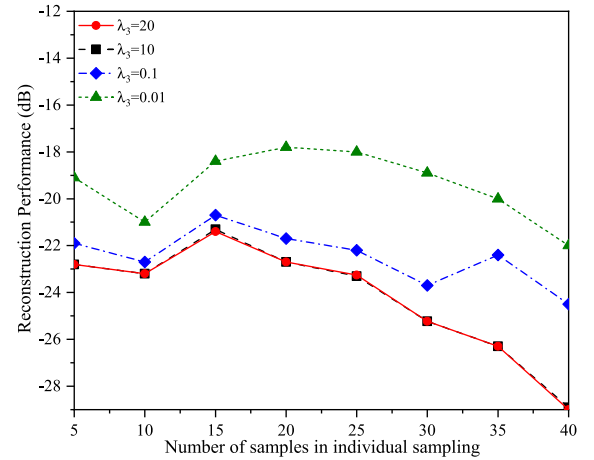


Fig. 10. Reconstruction performances of the noisy signal (SNR=25 dB) with different weights.

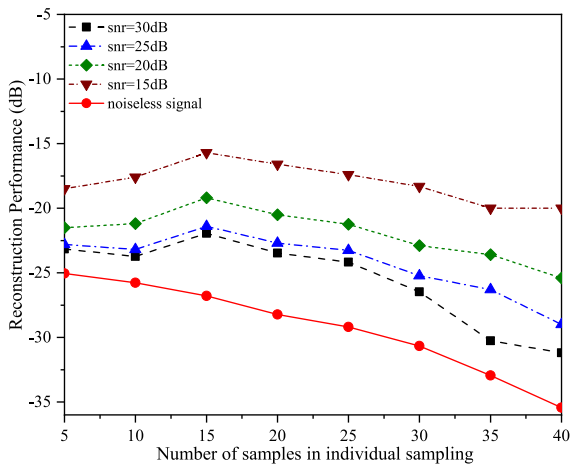


Fig. 9. Reconstruction performances with different noise levels.

time latency to collect and reconstruct the sensor data. For the proposed algorithms, the performance with eigen-vectors is close to that by random sampling scheme.

We further evaluate our proposed optimal sampling and reconstruction algorithms on different levels of noisy signals. The SNR ranges from 15 dB to 30 dB. We can observe from Fig. 9 that the proposed algorithms can well reconstruct the signals, which are robust to the noise. For noisy signals, the noise may be reduced by adding all the 4 graph signals together, and the joint frequency support is thereafter identified based on the combined signal. A bigger λ_3 will make f_3 defined in (88) plays a larger role in the signal reconstruction model, i.e., make the sum of estimated GFT coefficients of each signal close to the GFT coefficients of the combined signal, which may thereby help to improve the signal reconstruction performance. In Fig. 10, we show the reconstruction performances of noisy signals with SNR = 25 dB based on different weights, where λ_3 ranges from 0.01 to 20. We can observe that, in this example, to guarantee a good performance, λ_3 may not be too small, e.g., $\lambda_3 = 20$. However, the performance may not be significantly improved if the weight λ_3 is bigger than 20.

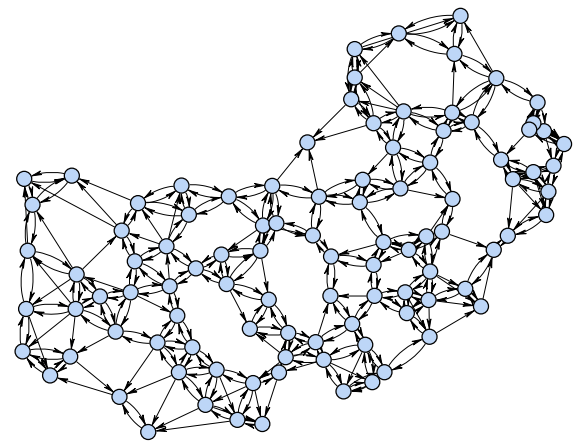


Fig. 11. Directed graph of sensor network with 100 vertices, where each sensor receives data from 4 nearest neighbour sensors.

C. Joint Sampling for Data Gathering in Sensor Networks: Directed Graph With $N = 100$

We further illustrate the proposed joint sampling and reconstruction algorithms on a larger dataset that measures the daily temperatures of $N = 100$ cities in South China [9]. The graph shift matrix \mathcal{S} is also constructed based on (91), and each sensor receives shifted signals from 4 nearest neighbour sensors. The directed graph is shown in Fig. 11. We consider 4 graph signals together for the joint sampling, and demonstrate the proposed optimal recovery algorithm over 360 days of measurements. The weights are given as $(\lambda_1, \lambda_2, \lambda_3, \lambda_4) = (1, 1, 0.1, 0.1)$. For noiseless signal, we can observe from Fig. 12 that the proposed optimal sampling and reconstruction outperform the sampling with random selection. Its reconstruction performance is also better than the aggregation sampling [36]. In this example, if the number of samples is larger than 30, randomized local aggregation [38] is better than aggregation sampling. The performances of Sobolev smoothness [48] and temporal difference smoothness [45] based methods are close to randomized

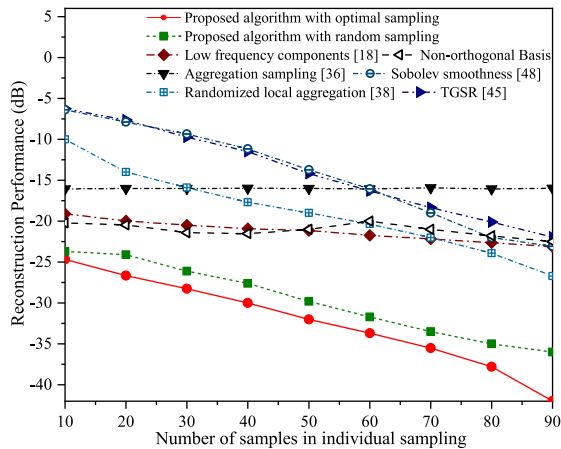


Fig. 12. Noiseless signal reconstruction over sensor network with unknown frequency support.

local aggregation method, which are repeated 20 times in the numerical studies. Since the proposed optimal algorithms can identify the frequency components associated with the largest GFT coefficient magnitudes, its performance is better than that in [18] using low-frequency components. The performance of the proposed algorithm using eigenvectors of the directed graph is close to the low-frequency components based method and can be improved by exploiting the orthogonality of Schur vectors in signal reconstruction.

D. Discussions of Computational Complexity

If we adopt the random sampling scheme, the computational complexity of the proposed algorithm would still be $O(N^3)$ according to Remark 4. Hence, the computational complexity may be the important limitation of the proposed method for signals over large directed graphs. Based on the authors' experience, the size of graph available for our proposed algorithms may be $N < 500$.

VIII. CONCLUSION

In this article, we investigate the sampling and reconstruction of multiple time-varying signals over directed graphs and show their applications in sensor network data gathering. Different from existing methods that employ smoothness property of signals in vertex domain, we consider signal reconstruction in two steps based on the assumption that the graph frequency supports of adjacent signals vary smoothly. Firstly, we design a two-stage Individual-Joint sampling scheme to identify the joint frequency support of the multiple varying signals by selecting the frequency components having the largest GFT coefficient magnitudes. Since the joint support is identified, each signal can be reconstructed using only a few data collected in individual sampling stage. Greedy algorithms are proposed for vertex set selection and graph shift order selection, which enable a robust signal reconstruction against additive noise because the minimum conditional number property is held in each step of the

greedy selection algorithms. For signals that are not strictly K -sparse in real applications, an optimal unbiased reconstruction method is proposed by fully exploiting the data collected in both individual and joint sampling stages, where the joint frequency support is selected adaptively and the signal reconstruction is considered as a convex optimization problem with the aid of the frequency components that are not included in the joint frequency support. We show that the proposed sampling and reconstruction methods can provide better performance than several existing algorithms in sensor network data gathering. Further study may be focused on the sampling of signals on dynamic graphs to adapt to the possible graph topology change in sensor network data gathering. For data analytics over large graphs, efforts may be dedicated to sampling and reconstruction-oriented graph partitioning.

APPENDIX

A. Proof of Lemma 1

Proof: Considering (2) together with (3), we have $\mathbf{u}_m^\ell = \mathbf{S}^\ell \mathbf{u}_m = \mathbf{Q}\mathbf{T}^\ell \hat{\mathbf{u}}_m$. Hence, (12) holds by sampling the ℓ -th order shifted signals on v_n , and (14)–(16) hold if we collect all the shifted signals for $\ell = 0, 1, \dots, L$ on v_n . Further collect shifted signals over the whole set \mathcal{V}_s , and notice that $\hat{\mathbf{u}}_m$ is K -sparse, then

$$\mathbf{u}_m^s = \Phi \hat{\mathbf{u}}_m = \Phi \Psi^T \hat{\mathbf{u}}_m^K \quad (92)$$

holds. To uniquely estimate all the nonzero GFT coefficients in $\hat{\mathbf{u}}_m^K$, the rank of matrix $\Phi \Psi^T$ should be equal to K . Hence, $\sigma L \geq K$ is required for (92). By multiplying vertex selection matrix \mathbf{C} on both sides of (92), and considering matrix Φ^K defined in (20), (21) holds if Φ^K is invertible. Constructing an invertible Φ^K will be discussed in Section V.

B. Proof of Proposition 1

Proof: Combine signals \mathbf{u}_m^s by (37) and according to (92),

$$\mathbf{u}^s = \Phi \hat{\mathbf{u}} \quad (93)$$

holds. The size of matrix Φ is σL -by- N . If the rank of Φ equals N , the combined GFT coefficients $\hat{\mathbf{u}}$ can be uniquely estimated. Hence, the number of sampled vertices σ and the maximum graph shifted order L should be designed to guarantee that $\sigma L \geq N$ and $\text{rank}(\Phi) = N$ hold. The vertex selection matrix \mathbf{C}_N is then performed on both sides of (93). If matrix Φ^N in (41) is invertible (which will be discussed in Section V-A), (42) is straightforward.

Since the combined signal \mathbf{u} is sparse, there are only $|\mathcal{S}|$ non-zero GFT coefficients in $\hat{\mathbf{u}}$. The frequency components corresponding to the non-zero GFT coefficients can hence be identified as the joint frequency support of the combined signal. This completes the proof. \square

REFERENCES

- [1] G. Mateos, S. Segarra, A. Marques, and A. Ribeiro, "Connecting the dots: Identifying network structure via graph signal processing," *IEEE Signal Process Mag.*, vol. 36, no. 3, pp. 16–43, May 2019.
- [2] S. Chen, Y. Eldar, and L. Zhao, "Graph unrolling networks: Interpretable neural networks for graph signal denoising," *IEEE Trans. Signal Process.*, vol. 69, pp. 3699–3713, 2021.
- [3] Z. Wang, M. Eisen, and A. Ribeiro, "Learning decentralized wireless resource allocations with graph neural networks," *IEEE Trans. Signal Process.*, vol. 70, pp. 1850–1863, 2022.
- [4] Y. Shen, G. Giannakis, and B. Baingana, "Nonlinear structural vector autoregressive models with application to directed brain networks," *IEEE Trans. Signal Process.*, vol. 67, no. 20, pp. 5325–5339, Oct. 2019.
- [5] S. Doshi and S. Chepuri, "Graph neural networks with parallel neighborhood aggregations for graph classification," *IEEE Trans. Signal Process.*, vol. 70, pp. 4883–4896, 2022.
- [6] V. Ioannidis, A. Marques, and G. Giannakis, "Tensor graph convolutional networks for multi-relational and robust learning," *IEEE Trans. Signal Process.*, vol. 68, pp. 6535–6546, 2020.
- [7] H. Wai, Y. Eldar, A. Ozdaglar, and A. Scaglione, "Community inference from partially observed graph signals: Algorithms and analysis," *IEEE Trans. Signal Process.*, vol. 70, pp. 2136–2151, 2022.
- [8] Z. Gao, F. Gama, and A. Ribeiro, "Wide and deep graph neural network with distributed online learning," *IEEE Trans. Signal Process.*, vol. 70, pp. 3862–3877, 2022.
- [9] X. Dong, D. Thanou, L. Toni, M. Bronstein, and P. Frossard, "Graph signal processing for machine learning: A review and new perspectives," *IEEE Signal Process Mag.*, vol. 37, no. 6, pp. 117–127, Nov. 2020.
- [10] Z. Xiao, H. Fang, and X. Wang, "Distributed nonlinear polynomial graph filter and its output graph spectrum: Filter analysis and design," *IEEE Trans. Signal Process.*, vol. 69, pp. 1725–1739, 2021.
- [11] Z. Xiao and X. Wang, "Nonlinear polynomial graph filter for signal processing with irregular structures," *IEEE Trans. Signal Process.*, vol. 66, no. 23, pp. 6241–6251, Dec. 2018.
- [12] F. Lozes, A. Elmoataz, and O. Lezoray, "PDE-based graph signal processing for 3-D color point clouds: Opportunities for cultural heritage," *IEEE Signal Process Mag.*, vol. 32, no. 4, pp. 103–111, Jul. 2015.
- [13] D. Shuman, S. Narang, P. Frossard, A. Ortega, and P. Vandergheynst, "The emerging field of signal processing on graphs: Extending high-dimensional data analysis to networks and other irregular domains," *IEEE Signal Process Mag.*, vol. 30, no. 3, pp. 83–98, May 2013.
- [14] A. Sandryhaila and J. Moura, "Big Data analysis with signal processing on graphs: Representation and processing of massive data sets with irregular structure," *IEEE Signal Process Mag.*, vol. 31, no. 5, pp. 80–90, Sep. 2014.
- [15] E. Bou-Harb, M. Debbabi, and C. Assi, "Big Data behavioral analytics meet graph theory: On effective botnet takedowns," *IEEE Netw.*, vol. 31, no. 1, pp. 18–26, Jan./Feb. 2017.
- [16] F. Chung and F. Graham, *Spectral Graph Theory*, vol. 92. Providence, Rhode Island, USA: Amer. Math. Soc., 1997.
- [17] A. Sandryhaila and J. Moura, "Discrete signal processing on graphs: Frequency analysis," *IEEE Trans. Signal Process.*, vol. 62, no. 12, pp. 3042–3054, Jun. 2014.
- [18] S. Chen, R. Varma, A. Sandryhaila, and J. Kovačević, "Discrete signal processing on graphs: Sampling theory," *IEEE Trans. Signal Process.*, vol. 63, no. 24, pp. 6510–6523, Dec. 2015.
- [19] M. Tsitsvero, S. Barbarossa, and P. Lorenzo, "Signals on graphs: Uncertainty principle and sampling," *IEEE Trans. Signal Process.*, vol. 64, no. 18, pp. 4845–4860, Sep. 2016.
- [20] A. Parada-Mayorga, D. Lau, J. Giraldo, and G. Arce, "Blue-noise sampling on graphs," *IEEE Trans. Signal Inf. Process. Netw.*, vol. 5, no. 3, pp. 554–569, Sep. 2019.
- [21] P. Li, N. Shlezinger, H. Zhang, B. Wang, and Y. Eldar, "Graph signal compression by joint quantization and sampling," *IEEE Trans. Signal Process.*, vol. 70, pp. 4512–4527, 2022.
- [22] T. Rautenberg, "Non-Bayesian estimation framework for signal recovery on graphs," *IEEE Trans. Signal Process.*, vol. 69, pp. 1169–1184, 2021.
- [23] G. Yang, L. Yang, Z. Yang, and C. Huang, "Efficient node selection strategy for sampling bandlimited signals on graphs," *IEEE Trans. Signal Process.*, vol. 69, pp. 5815–5829, 2021.
- [24] Y. Tanaka, "Spectral domain sampling of graph signals," *IEEE Trans. Signal Process.*, vol. 66, no. 14, pp. 3752–3767, Jul. 2018.
- [25] X. Wang, P. Liu, and Y. Gu, "Local-set-based graph signal reconstruction," *IEEE Trans. Signal Process.*, vol. 63, no. 9, pp. 2432–2444, May 2015.
- [26] P. Lorenzo, P. Banelli, E. Isufi, S. Barbarossa, and G. Leus, "Adaptive graph signal processing: Algorithms and optimal sampling strategies," *IEEE Trans. Signal Process.*, vol. 66, no. 13, pp. 3584–3598, Jul. 2018.
- [27] A. Anis, A. Gadde, and A. Ortega, "Efficient sampling set selection for bandlimited graph signals using graph spectral proxies," *IEEE Trans. Signal Process.*, vol. 64, no. 14, pp. 3775–3789, Jul. 2016.
- [28] F. Wang, G. Cheung, and Y. Wang, "Low-complexity graph sampling with noise and signal reconstruction via Neumann series," *IEEE Trans. Signal Process.*, vol. 67, no. 21, pp. 5511–5526, Nov. 2019.
- [29] A. Sakiyama, Y. Tanaka, T. Tanaka, and A. Ortega, "Eigendecomposition-free sampling set selection for graph signals," *IEEE Trans. Signal Process.*, vol. 67, no. 10, pp. 2679–2692, May 2019.
- [30] J. Shi and J. Moura, "Graph signal processing: Dualizing GSP sampling in the vertex and spectral domains," *IEEE Trans. Signal Process.*, vol. 70, pp. 2883–2898, 2022.
- [31] S. Chen, R. Varma, A. Singh, and J. Kovačević, "Signal recovery on graphs: Fundamental limits of sampling strategies," *IEEE Trans. Signal Inf. Process. Netw.*, vol. 2, no. 4, pp. 539–554, Dec. 2016.
- [32] H. Nguyen and M. Do, "Downsampling of signals on graphs via maximum spanning trees," *IEEE Trans. Signal Process.*, vol. 63, no. 1, pp. 182–191, Jan. 2015.
- [33] S. Chepuri and G. Leus, "Graph sampling for covariance estimation," *IEEE Trans. Signal Inf. Process. Netw.*, vol. 3, no. 3, pp. 451–466, Sep. 2017.
- [34] L. Chamon and A. Ribeiro, "Greedy sampling of graph signals," *IEEE Trans. Signal Process.*, vol. 66, no. 1, pp. 34–47, Jan. 2018.
- [35] A. Kroizer, T. Rautenberg, and Y. Eldar, "Bayesian estimation of graph signals," *IEEE Trans. Signal Process.*, vol. 70, pp. 2207–2223, 2022.
- [36] A. Marques, S. Segarra, G. Leus, and A. Ribeiro, "Sampling of graph signals with successive local aggregations," *IEEE Trans. Signal Process.*, vol. 64, no. 7, pp. 1832–1843, Apr. 2016.
- [37] G. Yang, L. Yang, and C. Huang, "An orthogonal partition selection strategy for the sampling of graph signals with successive local aggregations," *Signal Process.*, vol. 188, 2021, Art. no. 108211.
- [38] D. Valsesia, G. Fracastoro, and E. Magli, "Sampling of graph signals via randomized local aggregations," *IEEE Trans. Signal Inf. Process. Netw.*, vol. 5, no. 2, pp. 348–359, Jun. 2019.
- [39] E. Isufi, A. Loukas, N. Perraudin, and G. Leus, "Forecasting time series with VARMA recursions on graphs," *IEEE Trans. Signal Process.*, vol. 67, no. 18, pp. 4870–4885, Sep. 2019.
- [40] V. Ioannidis, Y. Shen, and G. Giannakis, "Semi-blind inference of topologies and dynamical processes over dynamic graphs," *IEEE Trans. Signal Process.*, vol. 67, no. 9, pp. 2263–2274, May 2019.
- [41] V. Ioannidis, D. Romero, and G. Giannakis, "Inference of spatio-temporal functions over graphs via multi-kernel kriged Kalman filtering," *IEEE Trans. Signal Process.*, vol. 66, no. 12, pp. 3228–3239, Jun. 2018.
- [42] F. Grassi, A. Loukas, N. Perraudin, and B. Ricaud, "A time-vertex signal processing framework: Scalable processing and meaningful representations for time-series on graphs," *IEEE Trans. Signal Process.*, vol. 66, no. 3, pp. 817–829, Feb. 2018.
- [43] J. Jiang, H. Feng, D. Tay, and S. Xu, "Theory and design of joint time-vertex nonsubsampling filter banks," *IEEE Trans. Signal Process.*, vol. 69, pp. 1968–1982, 2021.
- [44] S. Kadambari and S. Chepuri, "Product graph learning from multi-domain data with sparsity and rank constraints," *IEEE Trans. Signal Process.*, vol. 69, pp. 5665–5680, 2021.
- [45] K. Qiu, X. Mao, X. Shen, X. Wang, T. Li, and Y. Gu, "Time-varying graph signal reconstruction," *IEEE J. Sel. Topics Signal Process.*, vol. 11, no. 6, pp. 870–883, Sep. 2017.
- [46] F. Gama, A. Marques, G. Mateos, and A. Ribeiro, "Rethinking sketching as sampling: A graph signal processing approach," *Signal Process.*, vol. 169, 2020, Art. no. 107404.
- [47] J. Jiang, D. Tay, Q. Sun, and S. Ouyang, "Recovery of time-varying graph signals via distributed algorithms on regularized problems," *IEEE Trans. Signal Inf. Process. Netw.*, vol. 6, pp. 540–555, 2020.
- [48] J. Giraldo, A. Mahmood, B. Garcia-Garcia, D. Thanou, and T. Bouwmans, "Reconstruction of time-varying graph signals via Sobolev smoothness," *IEEE Trans. Signal Inf. Process. Netw.*, vol. 8, pp. 201–214, 2022.

- [49] J. Giraldo and T. Bouwmans, "On the minimization of Sobolev norms of time-varying graph signals: Estimation of new coronavirus disease 2019 cases," in *Proc. IEEE 30th Int. Workshop Mach. Learn. Signal Process.*, 2020, pp. 1–6.
- [50] A. Mondal, M. Das, A. Chatterjee, and P. Venkateswaran, "Recovery of missing sensor data by reconstructing time-varying graph signals," in *Proc. 30th Eur. Signal Process. Conf.*, 2022, pp. 2181–2185.
- [51] A. Sandryhaila and J. Moura, "Discrete signal processing on graphs," *IEEE Trans. Signal Process.*, vol. 61, no. 7, pp. 1644–1656, Apr. 2013.
- [52] G. Golub and C. Loan, *Matrix Computations*. Baltimore, MD, USA: Johns Hopkins Univ. Press, 2012.
- [53] S. Mollaebrahim and B. Beferull-Lozano, "Design of asymmetric shift operators for efficient decentralized subspace projection," *IEEE Trans. Signal Process.*, vol. 69, pp. 2056–2069, 2021.
- [54] S. Kay, *Fundamentals of Statistical Signal Processing: Detection Theory*, vol. 2. London, U.K.: Pearson, 2009.
- [55] Y. Chen, W. Li, and Y. Wang, "Online adaptive Kalman filter for target tracking with unknown noise statistics," *IEEE Sens. Lett.*, vol. 5, no. 3, Mar. 2021, Art. no. 1500404.
- [56] T. Strutz, *Data Fitting and Uncertainty*. Wiesbaden, Germany: Springer Vieweg, 2016.
- [57] M. Grant and S. Boyd, *Graph Implementations for Nonsmooth Convex Programs, Recent Advances in Learning and Control*, (Lecture Notes in Control and Information Sciences Series). Berlin, Germany: Springer-Verlag, 2008.
- [58] M. Grant and S. Boyd, "CVX: MATLAB software for disciplined convex programming, version 2.1," 2014. [Online]. Available: <http://cvxr.com/cvx>
- [59] H. Egilmez, E. Pavez, and A. Ortega, "Graph learning from filtered signals: Graph system and diffusion kernel identification," *IEEE Trans. Signal Inf. Process. Netw.*, vol. 5, no. 2, pp. 360–374, Jun. 2019.



Zhenlong Xiao (Member, IEEE) received the B.S. degree from the Nanjing University of Posts and Telecommunications, Nanjing, China, in 2008, the M.S. degree from the Beijing University of Posts and Telecommunications, Beijing, China, in 2011, and the Ph.D. degree from the Hong Kong Polytechnic University, Hong Kong, in 2015. He is currently an Associate Professor with the Department of Information and Communication Engineering, School of Informatics, Xiamen University, Xiamen, China. He was a Visiting Professor with the Department of

Electrical and Computer Engineering, Western University, London, ON, Canada in 2020. His research interests include graph signal processing, decentralized optimization, and nonlinear signal processing.



He Fang (Member, IEEE) received the Ph.D. degree in electrical and computer engineering from Western University, London, ON, Canada, in 2020. She is currently a Full Professor with the School of Electronic and Information Engineering, Soochow University, Suzhou, China. Her research interests include intelligent security provision, zero trust security, integrated sensing and communications. She is currently the Guest Editor and Topical Advisory Panel Member for several journals, including IEEE WIRELESS COMMUNICATIONS.

She was involved in many IEEE conferences including IEEE GLOBECOM, VTC, and ICC, in different roles such as the Session Chair and TPC Member. She was the Vice-Chair of Communication/Broadcasting Chapter, IEEE London Section, Canada, from September 2019 to August 2021.



Stefano Tomasin (Senior Member, IEEE) received the Ph.D. degree from the University of Padova, Padua, Italy, in 2003. During his studies he did internships with IBM Research, Switzerland and Philips Research, The Netherlands. He joined the University of Padova where he was an Assistant Professor from 2005 to 2015, an Associate Professor during 2016–2022, and has been a Full Professor since 2022. He was a Visiting Faculty with Qualcomm, San Diego, CA, USA, in 2004, the Polytechnic University, Brooklyn, NY, USA, in 2007 and the Mathematical

and Algorithmic Sciences Laboratory of Huawei, Paris, France, in 2015. His research interests include physical layer security, security of global navigation satellite systems, signal processing for wireless communications, synchronization, and scheduling of communication resources. He has been a Senior Member of IEEE since 2011 and member since 1999 and a member of EURASIP since 2011. He has been the Editor of the IEEE TRANSACTIONS ON VEHICULAR TECHNOLOGIES during 2011–2016, of the IEEE TRANSACTIONS ON SIGNAL PROCESSING during 2017–2020, of the *EURASIP Journal of Wireless Communications and Networking* since 2011 and of the IEEE TRANSACTIONS ON INFORMATION FORENSICS AND SECURITY since 2020. He has been the Deputy Editor-in-Chief of the IEEE TRANSACTIONS ON INFORMATION FORENSICS AND SECURITY since January 2023.



Gonzalo Mateos (Senior Member, IEEE) received the B.Sc. degree in electrical engineering from the Universidad de la República, Montevideo, Uruguay, in 2005, and the M.Sc. and Ph.D. degrees in electrical engineering from the University of Minnesota, Minneapolis, MN, USA, in 2009 and 2011, respectively. He is currently an Associate Professor with the Department of Electrical and Computer Engineering, University of Rochester, Rochester, NY, USA, an Asaro Biggar Family Fellow in data science. He is also the Associate Director for Research with the

Goergen Institute for Data Science, University of Rochester. During 2013, he was a Visiting Scholar with the CS Department, Carnegie Mellon University, Pittsburgh, PA, USA. From 2004 to 2006, he was a Systems Engineer with Asea Brown Boveri, Uruguay. His research interests include statistical learning from complex data, network science, decentralized optimization, and graph signal processing.



Xianbin Wang (Fellow, IEEE) received the Ph.D. degree in electrical and computer engineering from the National University of Singapore, Singapore, in 2001. He is currently a Professor and Tier-1 Canada Research Chair, Western University, London, ON, Canada. Prior to joining Western, he was with Communications Research Centre Canada, as a Research Scientist/Senior Research Scientist between July 2002 and December 2007. From January 2001 to July 2002, he was a System Designer with STMicroelectronics. His research interests include 5G/6G

technologies, Internet-of-Things, communications security, machine learning and intelligent communications. He has more than 600 highly cited journal and conference papers, in addition to 30 granted and pending patents and several standard contributions. Dr. Wang is a Fellow of Canadian Academy of Engineering, a Fellow of Engineering Institute of Canada, an IEEE Distinguished Lecturer. He was the recipient of many prestigious awards and recognitions, including IEEE Canada R.A. Fessenden Award, Canada Research Chair, Engineering Research Excellence Award at Western University, Canadian Federal Government Public Service Award, Ontario Early Researcher Award and six IEEE Best Paper Awards. He was the Editor-in-Chief, Associate Editor-in-Chief, Editor/Associate Editor for more than ten journals. He was involved in many IEEE conferences including GLOBECOM, ICC, VTC, PIMRC, WCNC, CCECE and CWIT, in different roles such as the General Chair, Symposium Chair, Tutorial Instructor, Track Chair, Session Chair, TPC Co-Chair and Keynote Speaker. He has been nominated as an IEEE Distinguished Lecturer several times during the last ten years. Dr. Wang was the Chair of IEEE ComSoc Signal Processing and Computing for Communications (SPCC) Technical Committee and is currently is the Central Area Chair of IEEE Canada.